Research Article

Bioinformatics and Biology Insights
Volume 19: 1–20

DOI: 10.1177/11779322251331104
journals.sagepub.com/home/bbi
Sage

A Reverse Vaccinology and Immunoinformatic Approach for the Designing of a Novel mRNA Vaccine Against Stomach Cancer Targeting the Potent Pathogenic Proteins of *Helicobacter pylori*

Abanti Barua[1], Md. Habib Ullah Masum[2] and Ahmad Abdullah Mahdeen[1]

Abstract

Helicobacter pylori infection of the stomach's epithelial cells is a significant risk factor for stomach cancer. Various *H pylori* proteins (CagA, GGT, NapA, PatA, urease, and VacA) were targeted to design 2 messenger RNA (mRNA) vaccines, V1 and V2, using bioinformatics tools. Physicochemical parameters, secondary and tertiary structure, molecular docking and dynamic simulation, codon optimization, and RNA structure prediction have also been estimated for these developed vaccines. Physicochemical analyses revealed that these developed vaccines are soluble (GRAVY <0), basic (pI <7), and stable (aliphatic index <80). The secondary and tertiary structure of the vaccines demonstrated robustness. The docking with toll-like receptors (TLRs) revealed that the vaccines have a potential affinity for TLR-2 (V1: −1132.3 kJ/mol, V2: −1093.6 kJ/mol) and TLR-4 (V1: −1042.7 kJ/mol, V2: −1201.2 kJ/mol), and molecular dynamics simulations confirmed their dynamic stability. Structural analyses of V1 (−505.96 kcal/mol) and V2 (−634.92 kcal/mol) mRNA vaccines underscored their stability. In addition, the vaccine showed a considerable rise in the counts of B cells and extended activation of both T cells was also observed for the vaccines, suggesting the potential for long-lasting immunity, and offering enhanced protection against *H pylori*. These findings not only suggest potential long-lasting immunity against *H pylori* but also offer hope for the future of stomach cancer prevention. Notably, the study emphasizes the need for subsequent animal and human-based studies to confirm these promising results.

Keywords

In silico-based vaccine, stomach cancer vaccine, *Helicobacter* pylori vaccine, reverse vaccinology

Received: 30 August 2024; accepted: 14 March 2025

Introduction

Stomach cancer, often known as gastric cancer, originates in the epithelial cells that line the stomach.[1] It ranks as the fifth most prevalent cause of cancer-related fatalities globally.[2] Stomach cancer includes various types, such as adenocarcinoma, gastrointestinal stromal tumors, neuroendocrine tumors, lymphomas, and squamous cell carcinoma.[3] Adenocarcinoma is the most common among these, accounting for approximately 90% of cases.[3] Multiple risk factors contribute to the development of stomach cancer, while *Helicobacter pylori* infection of the stomach's mucosal layer is a significant predisposing factor. This bacterium is responsible for several infections affecting the lymph tissue of the mucosa and causing ulcers and carcinoma.[4] The infectious factors of *H pylori* lead to prolonged inflammation that causes necrosis, lesions of tissue finally stomach cancer.[5] Based on the GLOBOCAN 2020 predictions, stomach cancer resulted in roughly

[1]Department of Microbiology, Noakhali Science and Technology University, Noakhali, Bangladesh
[2]Department of Genomics and Bioinformatics, Faculty of Biotechnology and Genetic Engineering, Chattogram Veterinary and Animal Sciences University, Khulshi, Chattogram, Bangladesh

Corresponding Author:
Abanti Barua, Department of Microbiology, Noakhali Science and Technology University, Noakhali 3814, Bangladesh.
Email: abantika2005@gmail.com

800 000 deaths, which is 7.7% of all cancer-related deaths. In 2020, there were approximately 1.1 million newly diagnosed cases of stomach cancer, which constituted 5.6% of all reported cancer cases.[6] In 2024, there are 26 890 new cases and 10 880 fatalities, representing 1.3% and 1.8% of total cancer cases and deaths, respectively.[7] The majority of stomach cancer cases, mostly 60%, were identified in Eastern Asia, with China contributing to 43.9% of these cases. In 2020, stomach cancer was reported as the predominant cancer diagnosed in 7 Asian countries: Iran, Afghanistan, Turkmenistan, Uzbekistan, Tajikistan, Kyrgyzstan, and Bhutan.[2] In the year 2020, the number of fatalities and incidents of stomach cancer in North America were 29 772 and 13 391, respectively, whereas South America had 49 547 cases and 39 165 deaths. In Central and Eastern Europe, there were around 65 516 cases that were confirmed to have led to 50 018 fatalities. On the contrary, Australia and New Zealand claimed to have recorded 2676 cases of stomach cancer with 1355 deaths. In Northern Africa, there have been approximately 93 977 confirmed cases and, however, 7727 fatalities.[8] Stomach cancer, however, is a highly deadly kind of cancer, with a 5-year survival rate of $<20\%$.[2,9] Since *H pylori* is responsible for nearly 90% of all cases of noncardia stomach cancer, there are no successful vaccine candidates against *H pylori* developed yet.[10]

Cancer vaccines have the potential to revolutionize cancer prevention and therapy by using the immune system of the body to identify and destroy cancer cells. Vaccines, as opposed to conventional therapies such as chemotherapy or radiation, can specifically target cancer cells while preserving healthy tissue, hence minimizing the likelihood of adverse consequences.[11] Although therapeutic cancer vaccines have only been used in a restricted number of clinical applications, this field of study continues to be dynamic, and there are a variety of approaches by which these vaccines can be administered. There are 3 categories of cancer vaccines: (1) cell-based vaccines, (2) protein/peptide-based vaccines, and (3) nucleic acid–based vaccines, which include DNA and RNA vaccines.[11] Cell-based vaccines consist of autologous or allogeneic whole tumor cells or autologous dendritic cells (DCs).[12] To create a tailored immune response that targets the cancer, autologous tumor cell vaccines use cancer cells extracted from the own tissues of patients. One benefit of this vaccine is that it can expose the patient's immune system to their unique tumor-associated antigens (TAAs), eliminating the requirement to recognize individual TAAs beforehand. This method, however, depends on collecting enough tumor samples, which is not usually possible until the cancer of a patient has progressed past a certain stage. Meanwhile, allogeneic tumor vaccines usually use a small number of well-established tumor cell lines, which aid in the standardization and scalability of cellular vaccine manufacturing.[13] In addition, TAAs are the main target of protein/peptide vaccines, which intend to stimulate the immune system in response to TAAs that express distinctively or more abundantly in malignant cells than in healthy ones.[14] Considering the nature of TAAs, their immunogenicity is often limited. Various strategies have been explored to circumvent this challenge and boost the effectiveness of protein or peptide vaccines. These approaches involve using inflammatory adjuvants during administration and combining the vaccines with additional immunostimulants, including toll-like receptor (TLR)-binding peptides.[15] However, protein/peptide vaccines need the pre-identification and precise targeting of specific antigens, which might prove particularly challenging for individuals with distinct mutations.[16]

The likelihood that viral infections might induce infected cells to synthesize virus-specific peptides limited to the major histocompatibility complex (MHC) class I/II has prompted research into viral-based vaccinations.[17] The use of viral vaccines is subject to some limitations, one of which pertains to the inherent immunological response of the body to counteract viral vectors.[18] Consequently, some researchers have endeavored to use a prime-boost approach, whereby an initial administration of a tumor antigen and viral vector is followed by a subsequent "boost" of the same antigen facilitated by an alternative viral vector.[19] Nucleic acid vaccines include DNA, RNA, and viral-based vaccines, which attempt to introduce genetic material into antigen-presenting cells (APCs), resulting in the translation of cancer-specific antigens or antigen fragments.[20] RNA vaccines predominantly employ messenger RNA (mRNA) that intends to stimulate the translation of antigens in APCs. One possible benefit of mRNA vaccines instead of DNA vaccines is their potential to culminate in fewer side effects or autoimmune diseases owing to their faster degradation. In addition, mRNA vaccines do not integrate into the genome, avoiding the emergence of additional oncogenic potential.[21] Moreover, mRNA vaccines have the advantage of being readily and expeditiously synthesized and manufactured, enabling rapid reactions to emerging infections or variations. Moreover, they induce prevailing immunological responses, including the production of antibodies and cellular immunity, leading to the development of a robust barrier against infection.[22]

The genome of *H pylori* consists of a circular DNA molecule with a length of 1 667 867 base pairs. It has a total of 1590 putative coding sequences.[23] Multiple virulence genes of *H pylori*, such as cytotoxin-associated gene A (CagA), vacuolating cytotoxin gene (VacA), gamma-glutamyl transpeptidase (GGT), neutrophil-activating protein A subunit (NapA), peptidoglycan O-acetyltransferase (PatA), and urease, have been associated with stomach cancer progression. The CagA encodes a protein (120-140 kDa) that enhances the pathogenicity of the bacterium by increasing the cytokine production (interleukin-8) level within the host cell.[24] In addition, CagA attaches itself to Grb2 through the area that contains EPIYA, causing an aberrant activation of the Ras signaling pathway that promotes aberrant cell proliferation.[25] The VacA encodes another virulence protein (87 kDa) that causes vacuolation in epithelial cells, resulting in cellular damage.[26] According to Hatakeyama,[27] a programmed necrosis pathway is responsible for the VacA-induced cell death of AZ-521 gastric epithelial cells. A virulence protein of *H pylori* is GGT, which leads to the consumption of glutamine and glutathione in the host cells, as well as the production of reactive oxygen species and

ammonia, thereby causing gastric epithelial cells to undergo necrosis, apoptosis, and cell-cycle arrest. In addition, via inducing cyclooxygenase-2, interleukin-8, inducible nitric oxide synthase, and peptides linked to epidermal growth factor, GGT may promote the proliferation of gastric epithelial cells and suppress cellular apoptosis and lead to cancer.[28] Oxidative stress in the gastric mucosa resulting from *H pylori* infection is a significant component that contributes to the development of gastric cancer.[29] Most *H pylori* strains contain the NapA gene, which encodes HP-NAP[30] that can activate neutrophils to generate reactive oxygen species (ROS)[31] and reactive nitrogen species (RNS), as well as to adhere to endothelial cells.[32] The ROS and RNS induced by *H pylori* can cause DNA damage and mutations that lead to the initiation of cancer.[33] The PatA of *H pylori* protects the bacterium from host lysozyme, thereby facilitating the immune evasion of the bacterium.[34] Besides, *H pylori* urease can contribute to the pathogenic activity of the bacterium by altering the host immune response through stimulating monocytes and polymorphonuclear leucocytes, resulting in inflammation and epithelial injury.[35] A recent study suggests that urease may increase the carcinogenic potential of *H pylori* by inducing HIF-1α,[36] which further plays a noncanonical role by reducing Cyclin D1 half-life, disrupting the cell cycle, and promoting angiogenesis.[37]

Considering the importance of these pathogenic proteins of *H pylori*, an effective mRNA vaccine against stomach cancer can be formulated. This type of vaccine, however, comprises multiple epitopes, including MHC-I, MHC-II, and B-cell epitopes from the pathogenic proteins of *H pylori*. As immunological stimulants against intracellular microorganisms or tumorigenic antigens, MHC-I molecules initiate the activation of cytotoxic T cells (TCs) when they engage with cytotoxic T lymphocytes (CTLs). Therefore, potential vaccines have been developed using the binding epitopes of MHC-I that trigger the activation of CD8+ T cells, which greatly aid in eradicating viral infections and tumorigenic antigens.[38] As an additional point of interest, MHC-II molecules present immunogenic processed peptides to the T-cell receptor (TCR) on CD4+ T cells. This is a critical stage in activating both cellular and antibody-mediated immune responses. When identifying developing cancers and rejecting transplants, the association between MHC-II molecules and TCR—which carry processed peptides—is fundamental.[39,40] Therefore, identifying the existence of CD4+ and CD8+ T cells is a crucial phase in developing an effective vaccine.[41,42] Also, B-cell epitopes play a pivotal role in the interactions between antigens and antibodies, therefore being an essential factor to consider when developing vaccines.[41,43]

The technique, known as "Reverse Vaccinology" (RV) and immunoinformatics, eliminates the necessity of cultivating pathogens.[44] The benefits of these approaches, which allow for vaccine research on organisms that are difficult or impossible to grow in a lab setting, continue to be attractive and decrease the time required for selecting target proteins by employing many species or strains simultaneously.[45] However, there are some cons, such as the accuracy of immunoinformatics predictions being contingent upon the sophistication of the algorithms employed and the data quality. Errors are frequently present in sequence data obtained from high-throughput analysis.[45] The mRNA vaccine and reverse vaccinology methods received considerable attention when the FDA issued emergency use authorization for the first 2 severe acute respiratory syndrome coronavirus-2 (SARS-CoV-2) mRNA vaccines—BNT162b2 from Pfizer/BioNTech and mRNA-1273 from Moderna. In addition, this groundbreaking work received the Nobel Prize in Physiology or Medicine in 2023.[46]

The study aims to design mRNA vaccine candidates against *H pylori* that might be utilized in reverse vaccinology to target stomach cancer. We utilized advanced immune-informatics methodologies to predict T helper lymphocyte (HTL), CTL, and B-lymphocyte epitopes predicted by the sequences of amino acids of the subsequent 6 proteins: CagA, GGT, NapA, PatA, urease, and VacA.

Materials and methods

Obtaining of sequence

The amino acid sequences of *H pylori* CagA (accession number: AAB58747.1), GGT (accession number: BDO45106.1), NapA (accession number: AAU21203.1), PatA (accession number: WP_308811605.1), urease (accession number: EJB13369.1), and VacA (accession number: AAU85846.1) were retrieved from National Center for Biotechnology Information (NCBI) protein database.[47] Subsequently, all the sequences underwent BLASTp (protein-protein BLAST) on the NCBI database. Next, the conserved sequences of each protein were used for all the subsequent steps (Figure 1).

Prediction of CTL epitopes

The CTL-binding epitopes of the selected proteins (CagA, GGT, NapA, PatA, urease, and VacA) were predicted using the Immune Epitope Database (IEDB)[48,49] and NetMHCIIpan 4.0 server,[48,50] using the default settings of the threshold for epitope identification, weight on TAP transport efficiency, and weight on C terminal cleavage. The CTLs recognize peptides presented by MHC-I molecules, and the peptide-binding groove of MHC-I is typically closed at both ends, accommodating peptides that are predominantly 8 to 10 amino acids in length, with 9-mers being the most common.[51] As a threshold, epitopes with a percentile rank ⩽1.0 and confined to 12 HLA alleles (HLA-A1, HLA-A2, HLA-A3, HLA-A24, HLA-A26, HLA-B7, HLA-B8, HLA-B27, HLA-B39, HLA-B44, HLA-B58, and HLA-B62) are classified as strong binders and thoroughly investigated. Subsequently, the antigenicity, allergenicity, and toxicity were assessed for each elected epitope by VaxiJen 2.0,[52] AllerTOP v. 2.0,[53] and ToxinPred server, respectively.[54,55]

Prediction of HTL epitopes

The HTL-binding epitopes of the retrieved proteins (CagA, GGT, NapA, PatA, urease, and VacA) were predicted by IEDB[48,56] and Net-MHC 4.0 server.[57] The default values

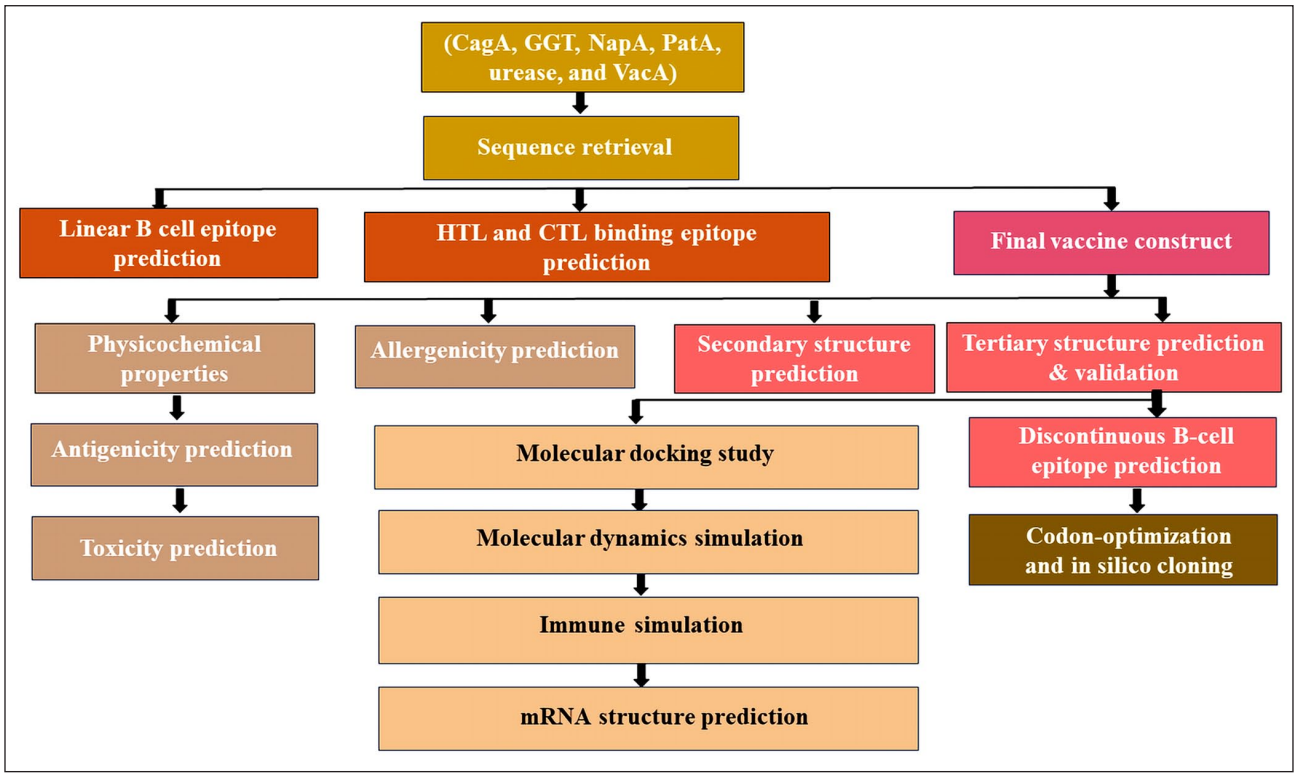

Figure 1. The outline of the entire study.

established the thresholds (percentile rank ⩽ 1.0) for strong and weak binders, while the epitopes were confined to 12 HLA-DRB alleles, including HLA-DRB1-0101, HLA-DRB1-0301, HLA-DRB1-0401, HLA-DRB1-0701, HLA-DRB1-0801, HLA-DRB1-0901, HLA-DRB1-1001, HLA-DRB1-1101, HLA-DRB1-1201, HLA-DRB1-1301, HLA-DRB1-1401, HLA-DRB1-1501, and HLA-DRB1-1601. The HTLs recognize peptides presented by MHC-II molecules. Unlike MHC I, the peptide-binding groove of MHC-II is open at both ends, allowing longer peptides, and thus, typically, 13 to 25 amino acids can be fitted with an optimal length of around 15-mer 51. Only those epitopes predicted by more than one allele were deemed strong binders and chosen for further study. Thereafter, the antigenicity, allergenicity, and toxicity were assessed for each elected epitope by VaxiJen 2.0,[52] AllerTOP v. 2.0,[53] and ToxinPred server, respectively.[54,55]

Prediction of linear B-cell epitopes

The linear B-cell epitopes of the protein of interest (CagA, GGT, NapA, PatA, urease, and VacA) were predicted by the IEDB[58] and ABCpred server.[59] The minimum score and maximum distance prediction parameters were set to 0.8 and 6 (Å), respectively. Afterward, the antigenicity, allergenicity, and toxicity were assessed for each elected epitope by VaxiJen 2.0,[52] AllerTOP v. 2.0,[53] and ToxinPred server, respectively.[54,55]

Population coverage of MHC alleles

The frequency of HLA alleles can fluctuate by geographic location and ethnicity.[60] Considering the population coverage of MHC alleles is essential in the development of a successful vaccine.[61] Using the IEDB (http://tools.iedb.org/population/), we employed the appropriate MHC alleles in conjunction with the targeted proteins' selected CTL and HTL epitopes, either individually or tandemly.[62]

Construction of the vaccine

The mapping of vaccine 1 (V1) and vaccine 2 (V2) was done using the highly prioritized epitopes of the selected proteins (CagA, GGT, NapA, PatA, urease, and VacA). The adjuvants, 50 S ribosomal protein L7/L12 and heparin-binding hemagglutinin (HBHA), were used as immune system enhancers in V1 and V2, respectively. The immune efficacy of a vaccine can be enhanced by adding L7/L12[63-65] and HBHA of *Mycobacterium tuberculosis* adjuvants, as demonstrated in laboratory trials.[63] Nevertheless, linkers are employed to distinguish epitopes, offering flexibility, cleavability, and stability to the epitopes inside the vaccine formulation.[63-65] In addition, the immunogenicity of a vaccine may be enhanced through the incorporation of linkers including AYY, EAAAK, AK, and KFER linkers, as these allow for intramolecular hydrogen bonding and preserve the individual functional properties.[63-65]

Assessment of biophysical qualities

The biophysical qualities of the V1 and V2, including the molecular mass, the overall count of amino acids, instability, aliphatic index, isoelectric point, overall mean of water solubility (GRAVY), the total count of positive and negative charged residues, and the total count of atoms, were predicted by Expasy's ProtParam server.[66,67] In addition,

the solubility of both vaccines was indicated by the SOSUI and SOLpro servers.[68-72] The allergenicity of both vaccines was evaluated by AllergenFP v.1.0,[73] AllerCatPro v.2.0,[74] and AlgPred servers.[72,75] Moreover, the antigenicity of both vaccines was also analyzed by ANTIGENpro and VaxiJen 2.0 server.[76]

Prediction of secondary structure

The prediction of secondary structures of the V1 and V2 were conducted by 3 servers including GOR4,[77] SOPMA,[72] and PSIPRED by keeping all the parameters at a default.[78-80]

Prediction, refinement and validatio n of the tertiary structure

The prediction of tertiary structures of the V1 and V2 were conducted employing I-TASSER server.[81] Next, a refinement was performed on the GalaxyWEB server for both vaccines.[82] Subsequently, the validation of both structures was performed utilizing the SAVES v6.0 server, which elucidates the quality of the predicted structures through the application of the Ramachandran plot and ERRAT analysis.[83-86]

Identification of discontinuous B-cell epitopes

The identification of discontinuous B-cell epitopes of the V1 and V2 was conducted by the DiscoTope 2.0[87] and Ellipro server by setting all the parameters at default.[88]

Binding affinity evaluation by molecular docking

Toll-like receptors are integral to the innate immune system, recognizing pathogen-associated molecular patterns (PAMPs) and initiating immune responses.[89] Among the TLR family, toll-like receptor-2 (TLR-2) and toll-like receptor-4 (TLR-4) are frequently utilized in vaccine design due to their specific ligand recognition and pivotal roles in immune activation compared with other receptors.[89,90] TLR-2 and TLR-4 recognize various PAMPs, making them versatile targets for various vaccine antigens.[89] In addition, binding these receptors leads to robust immune responses, essential for effective vaccine efficacy.[89,90] Prior to the docking, the human TLR-2 (PDB: 2Z7X) and human TLR-4 (PDB: 3FXI) tertiary structures were obtained from the Protein Data Bank (www.rcsb.org). Therefore, the CLUSPRO 2.0 server was utilized to check the binding affinity of both vaccines with TLRs.[91,92] However, PyMOL software and the PDBsum server were employed for the visualization and analysis of the complexes.[93]

Simulation of the molecular dynamics

The docked complexes of both vaccines and the free structure of both vaccines underwent simulation of the molecular dynamics through the GROningen MAchine for Chemical Simulations (GROMACS) (version 2022.3).[94] The GROMOS96 43a1 force field was employed for the simulation, utilizing the SPC water model to construct a cubic water box. The systems were neutralized with NaCl. A 50 ns molecular dynamics simulation was conducted using isothermal-isochoric (NVT) and isobaric (NPT) equilibration types, with a temperature of 300 K, a pressure of 1.0 bar, periodic boundary conditions, and a time integration step of 2 fs. The trajectory data were evaluated at a snapshot interval of 100 picoseconds. The root mean square deviation (RMSD), root mean square fluctuation (RMSF), radius of gyration (Rg), and solvent accessible surface area (SASA) were computed using the corresponding modules incorporated in the GROMACS program.

Optimization and cloning of the DNA of the vaccine

The Java Codon Adaptation Tool (JCat) server was used for codon optimization of the vaccine using the *Escherichia coli* strain K12.[95] The server determines a protein's codon adaptation index (CAI) and GC contents to evaluate its expression level. The CAI value of >0.8 is deemed a satisfactory score, while $\geqslant 1.0$ represents the optimal score. The integrity of the mRNA sequence is improved by a higher GC content, which is attributed to the stronger stacking interaction between guanine (G) and cytosine (C) due to triple hydrogen bonds.[96] Furthermore, the increased GC content facilitates the efficient processing of mRNA.[97] The acceptable GC contents, however, can range from 30% to 70%.[41] However, the optimized vaccine DNA underwent cloning into the *E. coli* plasmid vector pET-28a(+), with BamHI, BglII, and NdeI restriction sites ligated to the N- and C-terminals of the vaccine sequences, respectively.

Simulation of the immune response of the vaccine

The simulation of the immune response after the administration of both V1 and V2 was performed on the C-ImmSim server.[98] Three vaccine doses are typically administered at 28-day intervals to assure a robust and durable immune response.[99,100] The antigen is introduced in the first dose, which primes the immune system, whereas the second dose augments the immune response, leading to increased levels of B and T cell activation, and the third dose reinforces long-term immunity by further amplifying and maturing the immune response.[99] The simulation run was executed with steps in time set to 1, 84, and 168 and with a simulation volume and steps of 50 and 1000, respectively.

Structure prediction of the mRNA

The RNAfold website (http://rna.tbi.univie.ac.at/cgi-bin/RNAWebSuite/RNAfold.cgi) was employed to predict the secondary structures of both the V1 and V2.[101] The server estimates the query mRNA structures' thermodynamically derived minimum free energy (MFE).[102,103] Subsequently, using the Biomodel server, the optimal DNA sequences of

Table 1. List of selected CTL epitopes from the protein sequences with their antigenicity, allergenicity, and toxicity.

Vaccine	Protein	Peptide (Epitope)	Percentile rank	Antigenicity	Allergenicity	Toxicity
V1	CagA	SSNKELVGK	0.02	0.8680 (Probable antigen)	Probable non-allergen	Non-toxic
	GGT	SEAVSAPRF	0.01	0.5844 (Probable antigen)	Probable non-allergen	Non-toxic
	NapA	KLQKSIWML	0.03	0.5844 (Probable antigen)	Probable non-allergen	Non-toxic
	PatA	KLQKSIWML	0.03	0.8293 (Probable antigen)	Probable non-allergen	Non-toxic
	Urease	IGFKIHEDW	0.13	0.8293 (Probable antigen)	Probable non-allergen	Non-toxic
	VacA	RVNNQVGGY	0.01	0.8293 (Probable antigen)	Probable non-allergen	Non-toxic
V2	CagA	GINPEWISK	0.02	1.2858 (Probable antigen)	Probable non-allergen	Non-toxic
	GGT	NADLSALGY	0.01	0.6326 (Probable antigen)	Probable non-allergen	Non-toxic
	NapA	EGDKVTVTY	0.05	1.6060 (Probable antigen)	Probable non-allergen	Non-toxic
	PatA	EGDKVTVTY	0.05	1.6060 (Probable antigen)	Probable non-allergen	Non-toxic
	Urease	ALAGEGLIV	0.2	0.5395 (Probable antigen)	Probable non-allergen	Non-toxic
	VacA	KVWRIQAGR	0.02	0.6726 (Probable antigen)	Probable non-allergen	Non-toxic

the V1 and V2 taken from the cloning step were converted into RNA (https://biomodel.uah.es/en/lab/cybertory/analysis/trans.htm).[104] Next, the RNAfold website was then used to validate and predict secondary structures based on these RNA sequences.

Results

Obtaining of sequence

This study obtained and applied the amino acid sequences of the following 6 proteins of *H pylori*, including CagA, GGT, NapA, PatA, urease, and VacA, for subsequent analysis.

Prediction of CTL epitopes

The CTL-binding epitopes of the following proteins, CagA, GGT, NapA, PatA, urease, and VacA were predicted by the IEDB database and Net-MHC 4.0 server. A total of twelve 9-mer length peptides were selected based on their percentile rank (⩽1.00) (Table 1). Nonetheless, the selected epitopes exhibited traits of antigenicity, non-allergenicity, and non-toxicity.

Prediction of HTL epitopes

The prediction of HTL epitopes of the targeted proteins (CagA, GGT, NapA, PatA, urease, and VacA) was conducted employing the IEDB and NetMHCIIpan 4.0 server. Twelve 15-mer peptides were predicted from the proteins that were chosen on the basis of the lowest possible percentile rank (⩽1.00), which explains the high affinity. However, antigenicity, non-allergenicity and non-toxicity properties were found on the chosen epitopes (Table 2).

Prediction of linear B-cell epitopes

The prediction of epitopes of linear B-cells from the chosen proteins (CagA, GGT, NapA, PatA, urease, and VacA) was conducted on the IEDB and the ABCpred servers. Twelve 16-mer epitopes were chosen along with antigenicity, non-allergenicity, and non-toxicity properties (Table 3).

Population coverage for MHC alleles

The population coverage of the combined CTL and HTL alleles was predicted to be 100% across the maximum regions, including Central America, South America, North America, Oceania, West Indies, North Africa, Central Africa, West Africa, East Africa, Europe, South Asia, and Northeast Asia (Supplementary Figure 1). Following that, Southeast Asia (99.98%) and Southwest Asia (99.99%) hit significant coverage (Supplementary Figure 1). However, South Africa has the lowest population coverage rate at 95.27% (Supplementary Figure 1).

Construction of the vaccine

Using the chosen epitopes, adjuvants, and linkers, 2 distinct vaccines were constructed. The adjuvant, specifically the 50S ribosomal protein L7/L12, was conjugated to V1 utilizing the EAAK linker. In contrast, the HTL, CTL, and linear B-cell epitopes were interconnected by the AYY, AK, and KFER linkers, respectively (Figure 2A). In the case of V2, the HBHA adjuvant was linked with the EAAK linker. Concurrently, the remaining epitopes, comprising the helper T-cell (HTL), cytotoxic T-cell (CTL), and linear B-cell epitopes, were interconnected utilizing AYY, AK, and KFER linkers, respectively (Figure 2B).

Assessment of biophysical qualities

The ExPASy ProtPram server was used to obtain the biophysical qualities of both V1 and V2. Based on the server, V1 comprised 425 amino acids with an isoelectric point of 8.77, whereas V2 consisted of 493 amino acids with an isoelectric point of 9.36. However, V1 and V2 had molecular masses of 46 803.57 Da and 54 623.78 Da, respectively. The instability indices of V1 and V2 were 19.95 and 36.31, respectively (threshold =< 40). The GRAVY of the V1 and V2 were predicted to be −0.271 and −0.605, respectively,

Table 2. List of selected HTL epitopes from the protein sequences with their antigenicity, allergenicity, IFN-γ and IL-10 inducing capability, and toxicity.

Vaccine	Proteins	Peptides (Epitope)	Percentile rank	Antigenicity	Allergenicity	Toxicity
V1	CagA	STGYYSLARENAEHG	0.01	1.0483 (probable antigen)	Probable non-allergen	Non-toxic
	GGT	VIDYNMNISEAVSAP	0.01	1.0483 (probable antigen)	Probable non-allergen	Non-toxic
	NapA	EGDKVTVTYADDQLA	0.2	1.0483 (probable antigen)	Probable non-allergen	Non-toxic
	PatA	YTDFFLTNFNLILKS	0.17	1.0483 (probable antigen)	Probable non-allergen	Non-toxic
	Urease	DIGIKDGKIAGIGKG	0.18	1.0483 (probable antigen)	Probable non-allergen	Non-toxic
	VacA	LKAKIIGYGNVSTGT	0.03	1.0483 (probable antigen)	Probable non-allergen	Non-toxic
V2	CagA	SPEPIYATIDDLGGP	0.04	1.0483 (probable antigen)	Probable non-allergen	Non-toxic
	GGT	AIGFALAVVHPAAGN	0.03	1.0483 (probable antigen)	Probable non-allergen	Non-toxic
	NapA	DAIVLFMKVHNFHWN	0.76	1.0483 (probable antigen)	Probable non-allergen	Non-toxic
	PatA	FWRRWHITLSRFLKE	0.17	1.0483 (probable antigen)	Probable non-allergen	Non-toxic
	Urease	KADIGIKDGKIAGIG	0.69	1.0483 (probable antigen)	Probable non-allergen	Non-toxic
	VacA	GNSFTSYKDSADRTT	0.04	1.0483 (probable antigen)	Probable non-allergen	Non-toxic

Table 3. List of selected linear B-cell epitopes with their toxicity, allergenicity, and antigenicity.

Vaccine	Proteins	Peptides (Epitope)	Toxicity	Allergenicity	Antigenicity
V1	CagA	GDLSYTLKVMGKKQTE	Non-toxic	Probable non-allergen	0.5185 (probable antigen)
	GGT	TVLQVISNVIDYNMNI	Non-toxic	Probable non-allergen	0.4584 (probable antigen)
	NapA	TRVKEETKTSFHSKDI	Non-toxic	Probable allergen	0.8208 (probable antigen)
	PatA	DMAIGIALFFNIKLPI	Non-toxic	Probable non-allergen	1.5230 (probable antigen)
	Urease	NKDMQDGVKNNLSVGP	Non-toxic	Probable non-allergen	1.0080 (probable antigen)
	VacA	VWRIQAGRGFNNFPHK	Non-toxic	Probable non-allergen	0.4629 (probable antigen)
V2	CagA	DGISQLREEYSNKAIK	Non-toxic	Probable non-allergen	0.5868 (probable antigen)
	GGT	THYSVADRWGNAVSVT	Non-toxic	Probable non-allergen	0.78057 (probable antigen)
	NapA	ELSNTAEKEGDKVTVT	Non-toxic	Probable non-allergen	1.7223 (probable antigen)
	PatA	PKTRERERERESENAP	Non-toxic	Probable non-allergen	1.4087 (probable antigen)
	Urease	VGPATEALAGEGLIVT	Non-toxic	Probable non-allergen	0.8793 (probable antigen)
	VacA	KDKPSNTTQNNANNNQ	Non-toxic	Probable non-allergen	1.3924 (probable antigen)

(threshold = < 0). Moreover, both V1 and V2 were further validated as water-soluble (SOSUI and SOLpro). The aliphatic indices of the V1 and V2 were predicted to be 84.33 and 76.23, respectively (Table 4). These determined the good thermostability of both vaccines (threshold = 50-80). Furthermore, both the V1 and V2 vaccines were anticipated to be non-allergenic, as indicated by AllergenFP v.1.0, AllerCatPro v.2.0, and AlgPred. In addition, they were identified as containing antigenic proteins, as assessed by ANTIGENpro and VaxiJen 2.0 (Table 4).

Prediction of secondary structure

The secondary structures of the V1 and V2 were evaluated employing the GOR4, SOPMA, and PSIPRED servers. For V1, the GOR4 provided 33.88% random coil, 50.35% alpha helix, and 15.76% extended strands (beta sheet). However, the SOPMA exhibited a random coil of 24.47%, an alpha helix of 44.71%, and extended strands of 21.18% in the secondary structure of V1 (Figure 3). For V2, the GOR4 demonstrated 24.14% random coil, 64.91% alpha helix, and 10.95% extended strands (beta sheet). However, the SOPMA predicted a random coil of 20.28%, an alpha helix of 59.43%, and extended strands of 14.40% in the secondary structure of V2 (Figure 3). Nevertheless, the PSIPRED provided the secondary structure characteristics of V1 and V2 through 3-state prediction, including coil, helix, and strands (Figure 4).

Prediction, refinement, and validation of tertiary structure

The I-TASSER was employed to predict the tertiary structure of both V1 and V2 by incorporating threading, fragment assembly, and refinement. A confidence score (C-score), which provides a measure of the quality of alignments and model compactness, was then used to rank the predicted models. In V1, 5 models were predicted but the model having the highest C-score of −1.35, TM-score of 0.55 ± 0.15, and RMSD of 10.1 ± 4.6Å was selected. In V2, the model having the highest C-score of −0.85, TM-score of 0.54 ± 0.15, and the RMSD of 8.1 ± 4.6Å was selected. Next, the refined model of V1 was taken from the GalaxyWEB server with RMSD, MolProbity score, and Ramachandran's favored region of 0.468, 2.093, and 91.7%, respectively (Figure 5A). Conversely, the refined model of the V2 exhibited an RMSD of 0.445, a MolProbity score of 2.808, and a Ramachandran-favored region percentage of 92.9% (Figure 5A). However, the Ramachandran plot depicted that the refined model of V1 had 85.5% amino

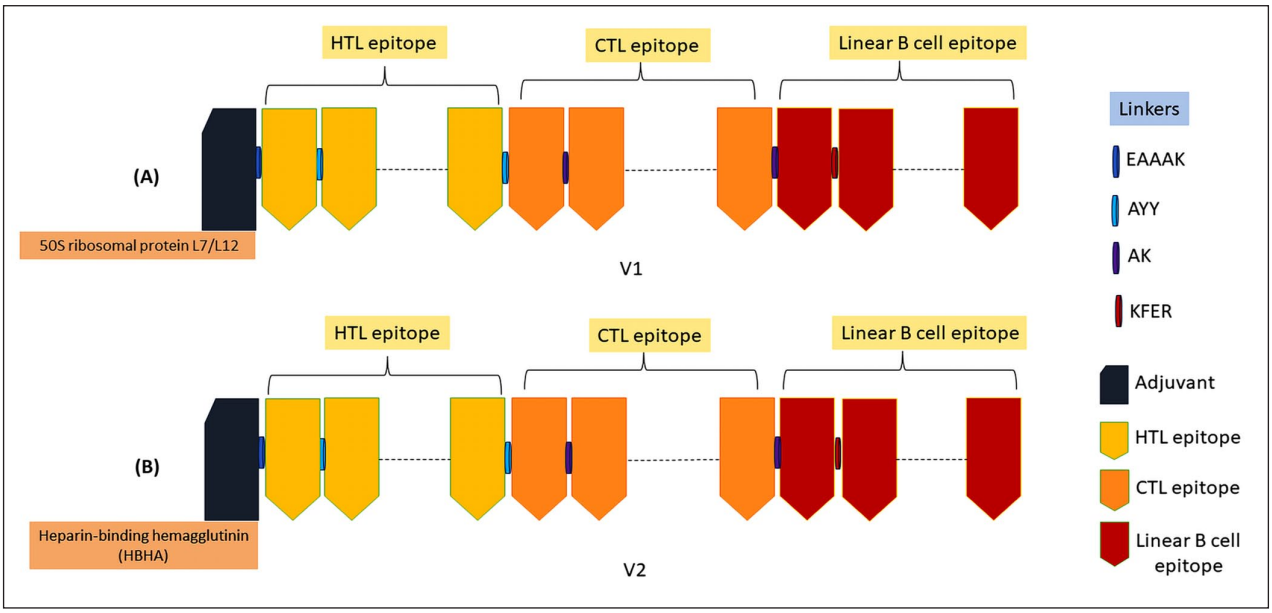

Figure 2. The construction of mRNA vaccines: V1 (A) and V2 (B). The illustration of the vaccines having adjuvant (deep blue color), epitopes (HTL—yellow, CTL—orange, linear B cell—maroon), and linkers (EAAAK—deep blue, AYY—light blue, AK—purple, KFER—maroon).

Table 4. The physicochemical and immunological properties of the V1 and V2.

Physicochemical properties	V1	V2
Molecular weight (Da)	46 803.57	54 623.78
Number of amino acids	425	493
Theoretical pI	8.77	9.36
GRAVY	−0.271	−0.605
Instability index	19.95 (stable protein)	36.31 (stable protein)
Aliphatic index	84.33	76.23
Total number of negatively charged residues (Asp + Glu)	57	68
Total number of positively charged residues (Arg + Lys)	62	82
Number of atoms	6641	7728
Solubility (SOSUI/SOLpro)	Soluble protein	Soluble protein
Allergenicity (AllergenFP v.1.0/ AllerCatPro v.2.0/ AlgPred)	Probable non-allergen	Probable non-allergen
Antigenicity (ANTIGENpro/VaxiJen 2.0)	Probable antigen (0.5965)	Probable antigen (0.6416)

acid residues in the most favored region, 11.5% in the additional allowed region, and 1.3% in the generously allowed region (Figure 5B). Moreover, the Ramachandran plot depicted that the refined model of V2 had 88.1% amino acid residues in the most favored region, 8.5% in the additional allowed region, and 1.1% in the generously allowed region (80 to >90%) (Figure 5B). The ERRAT score of the refined V1 was calculated to be 82.258, whereas, for the V2, it was calculated to be 90.683 (>50) (Figure 5C). In addition, the structure quality was further validated based on a Z score that resulted in −2.28 for V1 and −2.6 for V2 (−10 to 0).

Identification of discontinuous B-cell epitopes

A total of 225 discontinuous B-cell epitope residues were found in the V1 and V2 structures (Figure 6). In V1, the scores of epitopes were in 0.524 to 0.86 and 0.635 to 0.825 ranges, respectively, for V1 and V2 (Supplementary Table 1).

Binding affinity evaluation by molecular docking

From the 30 created models, the one exhibiting the central energy score of −868 kJ/mol and the lowest energy score of −1132.3 kJ/mol was chosen for the V1-TLR-2 complex, whereas the model with identical values of −1042.7 kJ/mol was picked for the V1-TLR-4 complex (Figure 7A, B and Table 5). Analogous to the V1, the model exhibiting the central energy score and the lowest energy score of −1006.7 and −1093.6 kJ/mol, respectively, was chosen for the V2-TLR-2 complex, whereas the model with center and lowest energy scores of −940.7 and −1201.2 kJ/mol, respectively, was picked for the V2-TLR-4 complex (Figure 7C, D and Table 5). Subsequently, the PDBsum predicted the

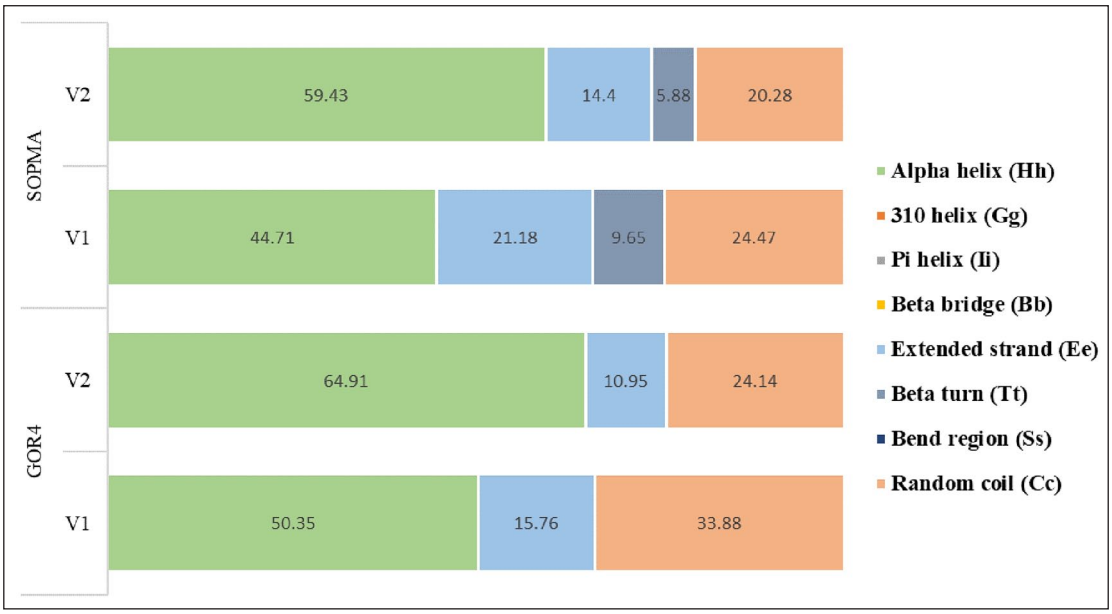

Figure 3. The secondary structure of the V1 and V2 predicted by GOR4 and SOPMA.

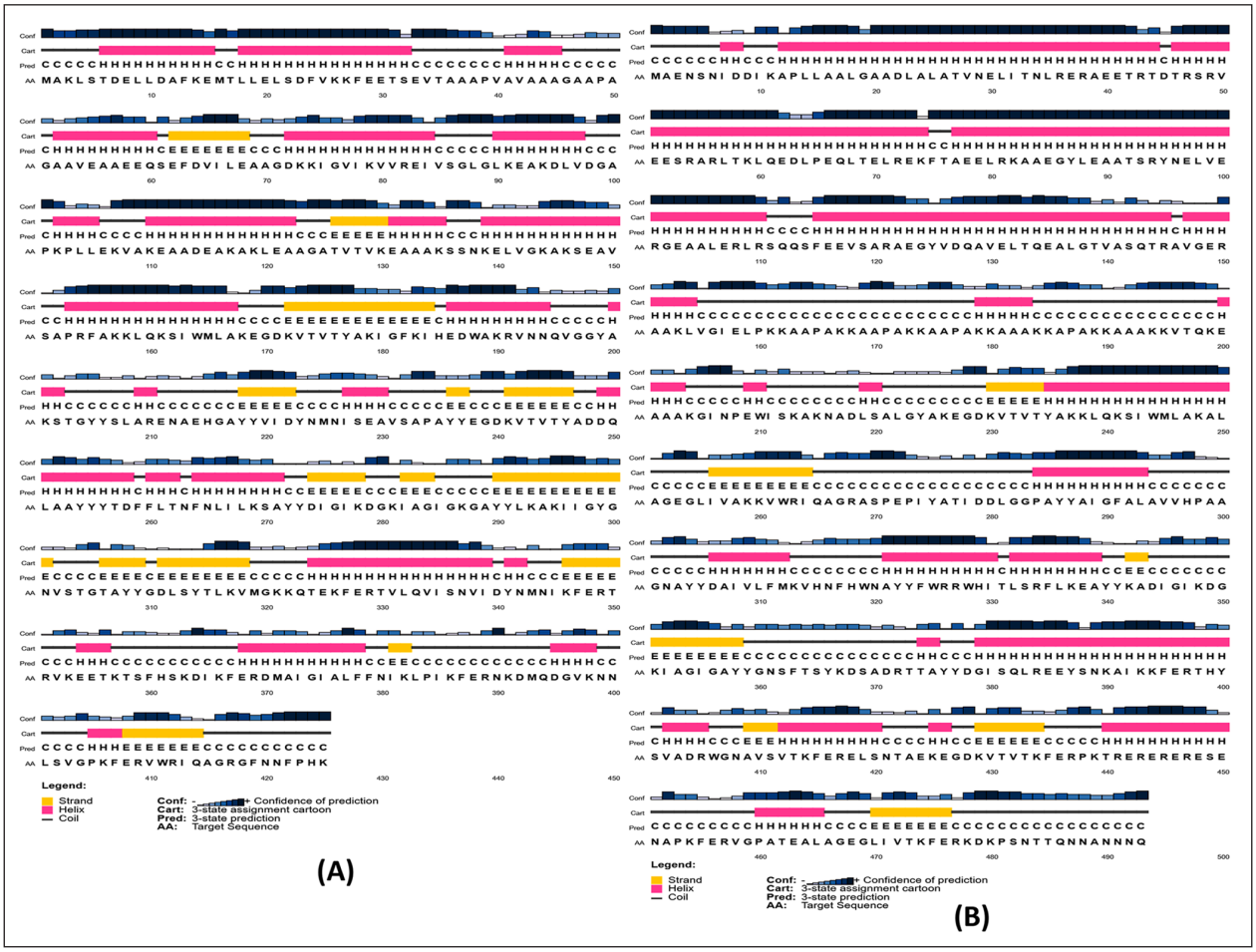

Figure 4. The predicted secondary structure for V1 (A) and V2 (B). The initial bar (Conf) represents the degree of confidence in the prediction, with the length of the bar denoting varying levels of assurance. In the following bar (Cart), the presence of beta-sheets is signified in yellow hue, the helical structure is denoted by pink hue, and the coil configuration is represented by gray hue. However, 3 distinct structural characteristics and corresponding amino acid sequences are depicted on the next 2 bars (Pred and AA).

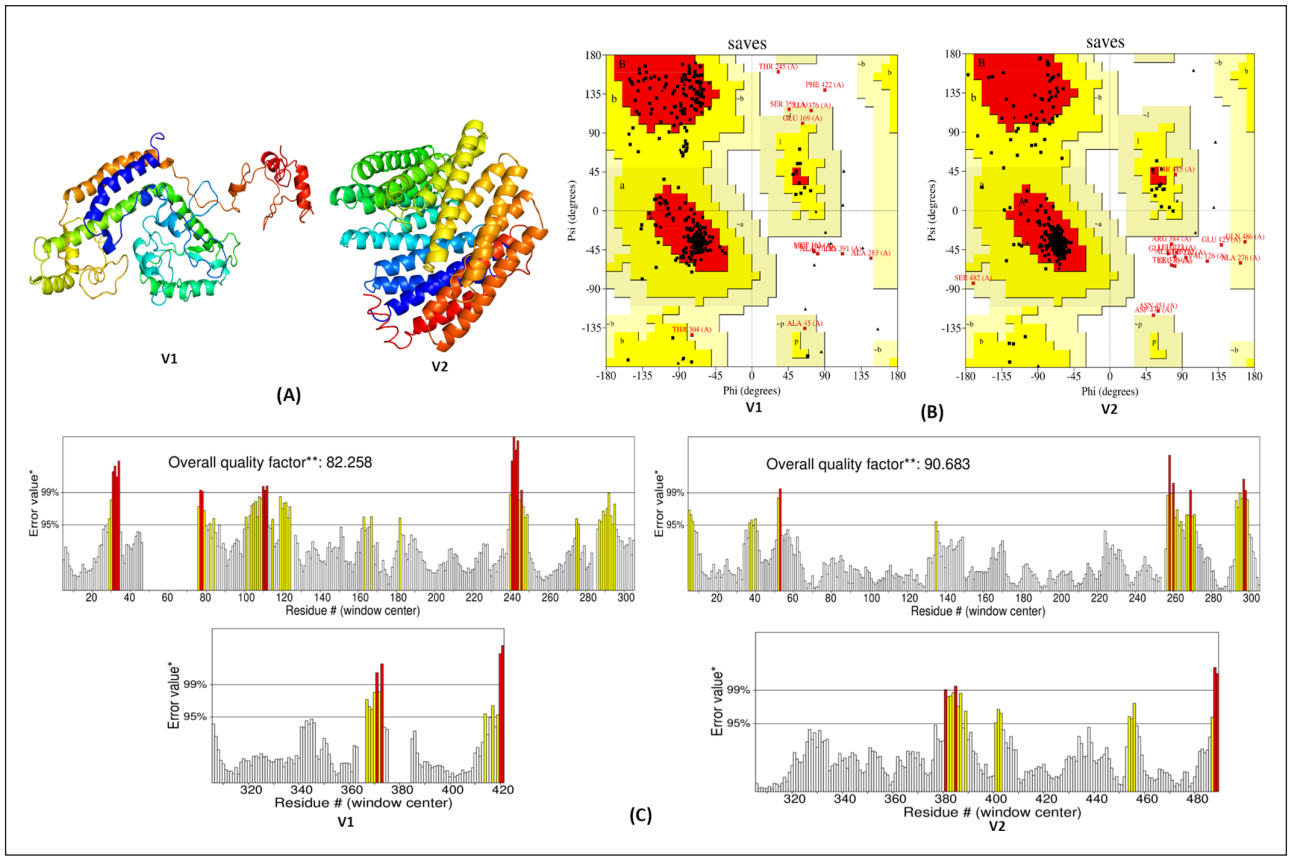

Figure 5. The prediction and validation of tertiary models of vaccines. The refined tertiary structures (A) are assessed employing Ramachandran plot score (B) and ERRAT (C) score.

number of hydrogen bonds, salt bridges, and non-bond interactions of 3, 7, and 166 in the V1-TLR-2 complex, respectively (Figure 7A and Table 5). However, the number of hydrogen bonds, salt bridges, and non-bond interactions were 8, 22, and 327 in the V1-TLR-4 complex, respectively (Figure 7B and Table 5). In addition, the number of hydrogen bonds, salt bridges, and non-bond interactions were 2, 10, and 182 in the V2-TLR-2 complex, respectively (Figure 7C and Table 5). However, the number of hydrogen bonds, salt bridges, and non-bond interactions were 12, 32, and 300 in the V2-TLR-4 complex, respectively (Figure 7D and Table 5).

Simulation of the molecular dynamics

Following a successful simulation, the RMSD of the vaccines (V1 and V2) and vaccine-TLR complexes (V1-TLR-2, V1-TLR-4, V2-TLR-2, and V2-TLR-4) was computed to assess structural stability. During the 50-ns simulation, the RMSD values for V1 and V1-TLR-4 exhibited a consistent increase; however, the RMSD values for V1-TLR-2 experienced a significant surge. Nevertheless, the RMSD of the complexes exhibited a tendency to diminish over a 50-ns simulation session (Figure 8A). The RMSD values for V2-TLR-2 and V2-TLR-4 exhibited a consistent increase, whereas the RMSD values for V1 remained unchanged. Conversely, the RMSD of the V2-TLR-2 and V2-TLR-4 began to decline once more following the 50-ns simulation session (Figure 8B). The RMSF of these complexes was used to evaluate regional flexibility. During the simulation, the motility pattern of V1-TLR-4 (Supplementary Figure 2C) markedly differs from that of V1-TLR-2 (Supplementary Figure 2B) and V1 apo (Supplementary Figure 2A), particularly at the C and N terminals. The motility pattern of RMSF for V2 apo (Supplementary Figure 2D) was significantly distinct from that of V2-TLR-2 (Supplementary Figure 2E) and V2-TLR-4 (Supplementary Figure 2F).

Throughout the simulation run, V1-TLR-4 had a greater Rg value than V1 and V1-TLR-2 (Figure 9A). Moreover, the Rg value of V2-TLR-4 was greater than that of V2 and V2-TLR-2 (Figure 9B). Throughout the whole simulation run, there was no significant difference in the SASA values of the V1 (Supplementary Figure 3A), V1-TLR-2 (Supplementary Figure 3B), and V1-TLR-4 (Supplementary Figure 3C) after 50 ns of running the simulation. The SASA values of the V2, V2-TLR-2, and V2-TLR-4 were also not significantly different during the simulation (Supplementary Figure 3D, Supplementary Figure 3E, and Supplementary Figure 3F, respectively).

Optimization and cloning of the DNA of the vaccine

According to the server, V1 and V2 had optimized DNA sequences of 1270 and 1473 nucleotide lengths, respectively. In addition, for both vaccines, the CAI values

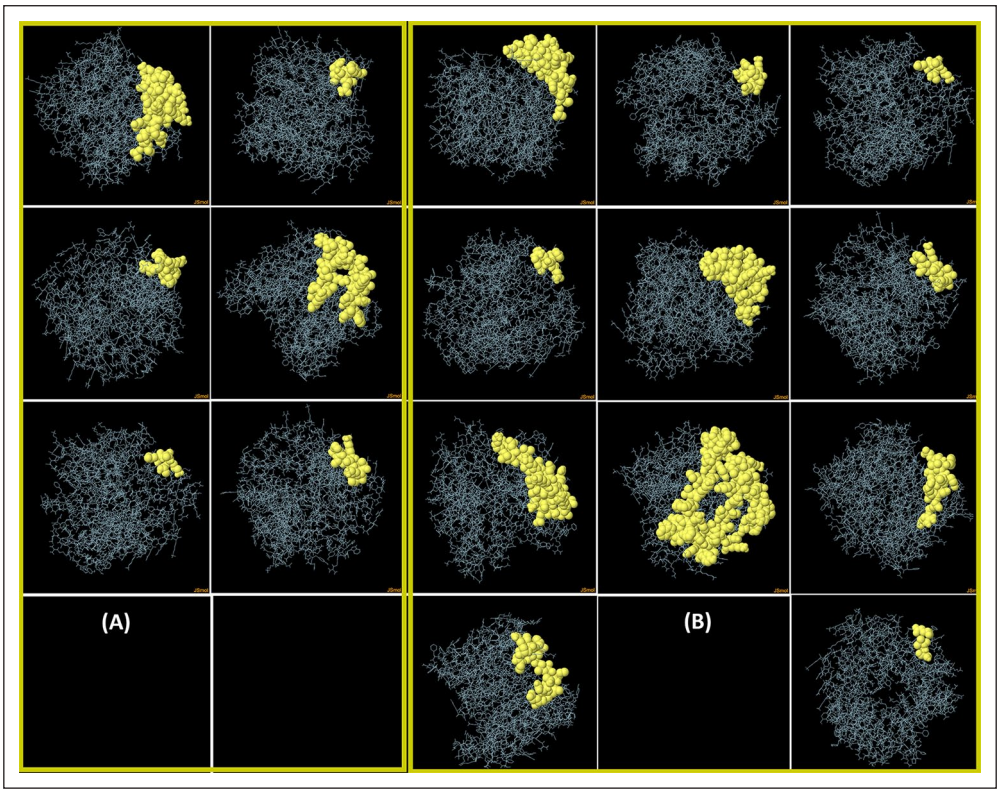

Figure 6. Tertiary representation of discontinuous B-cell epitopes of V1 (A) and V2 (B). The discontinuous B-cell epitopes are depicted in yellow-hue and the vaccine is depicted as gray sticks.

were determined to be 1.0. Moreover, the GC content was 51.23% and 51.50%, respectively, for V1 and V2 (Figure 10).

Simulation of the immune response of the vaccine

After 3 doses of administration, a significant rise in the counts of B cell was observed for both V1 (Figure 11A) and V2 (Figure 11B) vaccines, with the total B-cell counts remaining active, signifying persistent immunity over the course of a year (Figure 11A and B). Moreover, T cells were similarly apparent for V1 and V2 including an increased amount of active TH cells at day 60, which subsequently declined but persisted for nearly a year (Figure 11C and D). Moreover, active T cells demonstrated elevated expression following the vaccination regimen and continued to be stimulated for approximately 1 year (Figure 11E and F). In the case of both V1 and V2, vaccination also elicited cytokine responses, including interferon gamma (IFN-γ), which was at the highest uprising level and increased to nearly 2×10^6 Mg/mL. After 50 days, it decreased to 400 000 Mg/mL. Interleukin-12 and interleukin-10 were the lowest in this simulation, at approximately 50 000 mg/mL. Tumor growth factor-b was at >500 000 Mg/mL at 25 days and decreased at 50 days. The level of cytokines was initially found but vanished 100 days after the vaccination (Figure 11G and H).

Structure prediction of the mRNA

The secondary structure of the V1 mRNA demonstrated MFE score of −487.80 kcal/mol (optimum structure) and −354.19 kcal/mol (centroid structure). In contrast, V2 represented MFE score of −617.70 kcal/mol (optimum structure) and −515.48 kcal/mol (centroid structure). The thermodynamic free energy was found as −505.96 kcal/mol and −634.92 kcal/mol, respectively. In addition, there was a 0.00% correlation between the MFE structures of V1 and V2 in every ensemble (Figure 12).

Discussion

Among all cancers, stomach cancer ranks fifth in terms of mortality worldwide.[2] Most of these malignancies start as chronic gastritis by an infection with *H pylori*. A vaccine against this infection would be a significant weapon to prevent stomach cancer effectively.[105] Currently, no vaccine is commercially available for stomach cancer treatment.[106] Nevertheless, extensive research is being conducted on different types of cancer vaccines to explore their potential in combating stomach cancer. Various types of vaccines can be used to target cancer cells. These vaccines include peptide, DC, whole tumor cell, and checkpoint inhibitor vaccines.[106,107]

Epitope or peptide-based vaccines can also be developed to target overexpressed proteins or only found in cancer

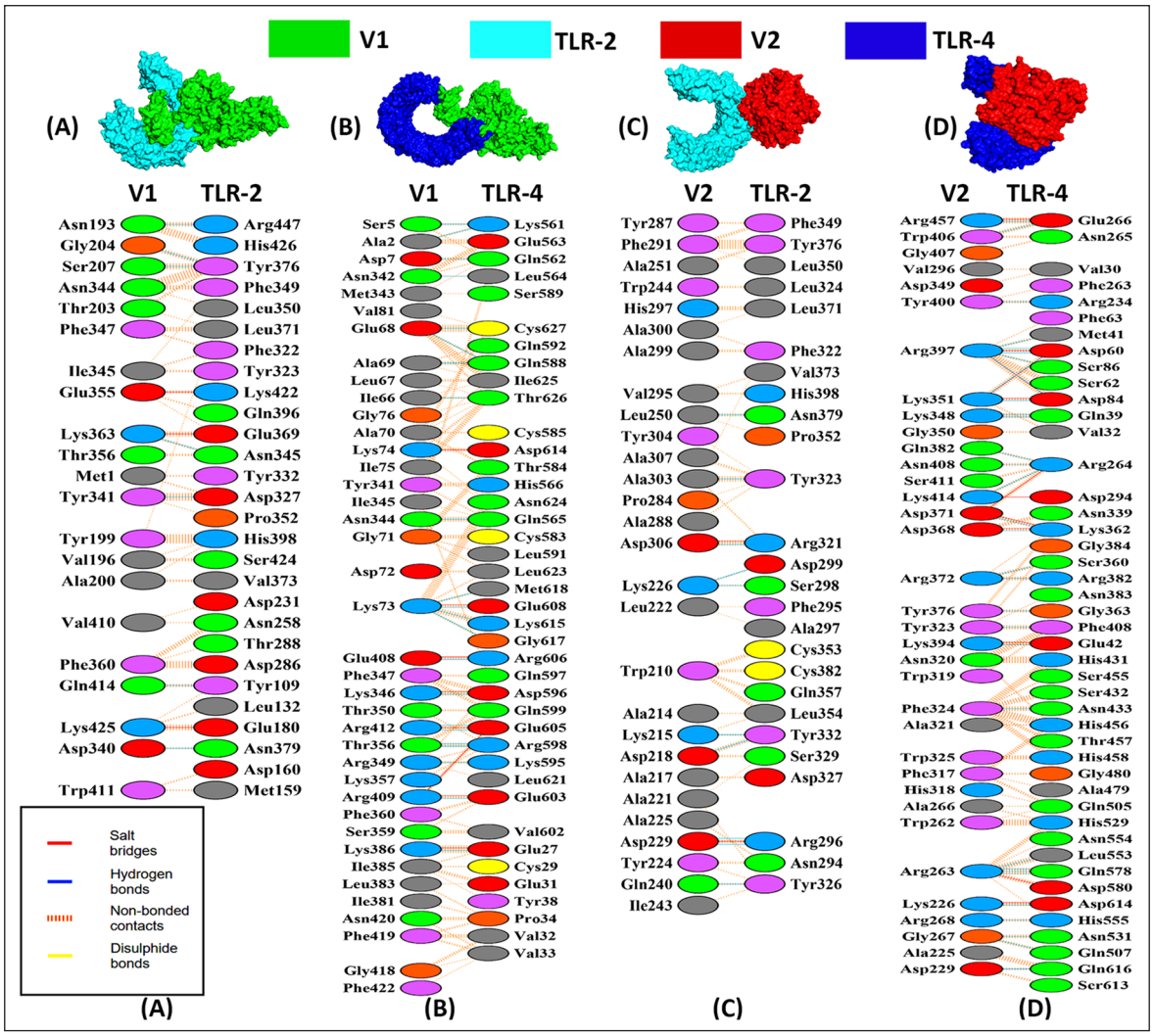

Figure 7. The binding interplay among the V1-TLR-2 (A), V1-TLR-4 (B), V2-TLR-2 (C), and V2-TLR-4 (D) complexes. The vaccines, V1 and V2, and the receptors, TLR-2 and TLR-4, are represented in green, red, cyan, and deep blue, respectively.

Table 5. The docking scores and interactions between the vaccine-receptor complexes.

		Weighted score, kJ/mol		Interactions of vaccine with TLRs		
Vaccine	Complex	Center	Lowest energy	Salt bridges	Hydrogen bonds	Non-bonded contacts
V1	Vaccine-TLR-2	−868	−1132.3	3	7	166
	Vaccine-TLR-4	−1042.7	−1042.7	8	22	327
V2	Vaccine-TLR-2	−1006.7	−1093.6	2	10	182
	Vaccine-TLR-4	−940.7	−1201.2	12	32	300

cells.[108] Although showing considerable perspective, these vaccines also pose particular challenges and constraints.[109] Identifying epitopes that induce a robust immune response against a wide range of cancer types can be challenging, potentially limiting the effectiveness of peptide-based vaccines.[109] In addition, peptide-based vaccines may not elicit a sufficiently strong and durable immune response, particularly in individuals with altered immune systems or in the context of tumor immune evasion mechanisms. Furthermore, the prerequisite for personalized vaccine formulations adds complexity to developing and implementing peptide-based vaccines.[110] Higashihara et al[111] conducted a phase I clinical trial to assess the safety of peptide vaccines with VEGFR1-A12-9 1084 and URLC10-A24-177 epitope peptides in patients with advanced stomach cancer who were chemo-resistant. This research indicates that administering URLC10 and VEGFR1 peptides by vaccination offers an effective therapeutic approach for advanced stomach cancer. Ishikawa et al[112] also designed a peptide vaccine against stomach cancer targeting the LY6K-177 peptide, which showed anticancer efficacy in stomach cancer patients after a phase I clinical trial. In a separate investigation, following

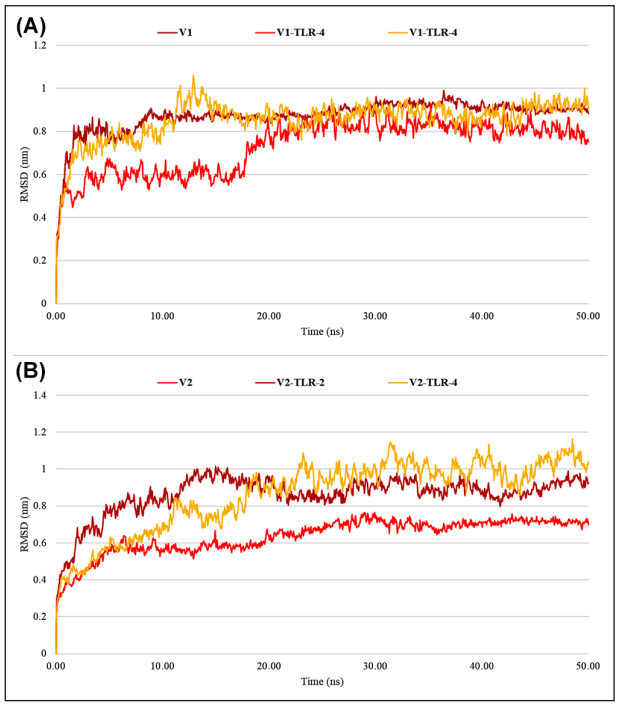

Figure 8. The RMSD analysis of the vaccines and vaccine-TLRs structures. The plot represents the RMSD of V1 and V1-TLRs (V1-TLR-2 and V1-TLR-4) (A), and V2 and V2-TLRs (V2-TLR-2 and V2-TLR-4) (B).

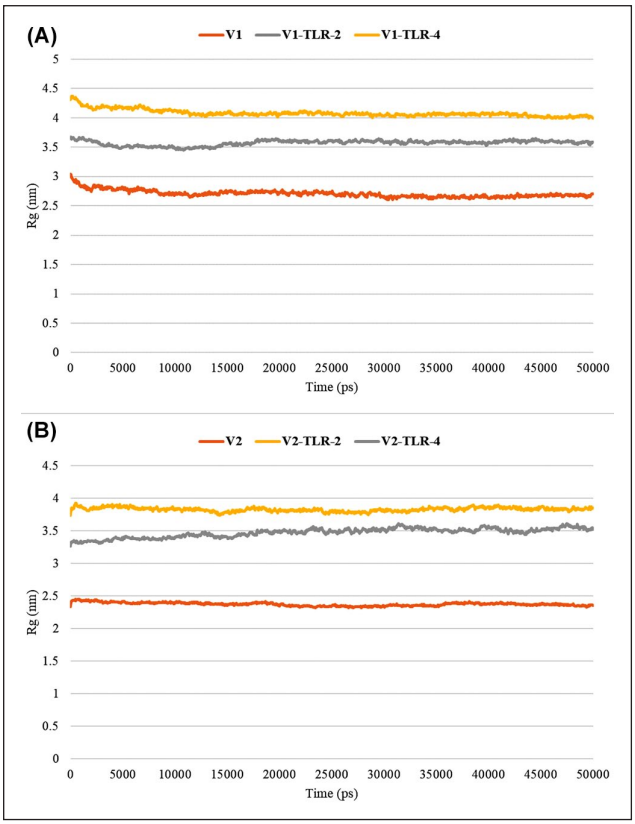

Figure 9. The RMSF analysis of the vaccines and vaccine-TLRs structures. The plot represents the RMSD of V1 and V1-TLRs (V1-TLR-2 and V1-TLR-4) (A), and V2 and V2-TLRs (V2-TLR-2 and V2-TLR-4) (B).

the administration of the HER2/DC vaccine to those who have advanced stomach cancer, the patient achieved remission with reduced levels of tumor markers. However, Moss et al[113] developed an epitope-based vaccine against *H pylori*–associated stomach cancer (Helicovaxor), which has shown promising therapeutic protection in mice in preclinical trial. In addition, Sichuan University (urease subunits) and Southern Medical University (Lp220) have recently demonstrated 2 epitope-based vaccines targeting the urease and Lp220 protein *H pylori*, which offer marginal protection to BALB/c mice in a preclinical trial.[114] Wuhu Kangwei Biological Technology Co., Ltd. presented phase III clinical data demonstrating the efficacy of an *H pylori* recombinant vaccine against natural infection and stomach cancer.[115,116]

Recent advances in the research of vaccinology have revealed that therapeutic agents based on mRNA have undergone significant advancements and may be able to overcome the challenges encountered while developing vaccinations for cancer and infectious diseases.[117] There are multiple mRNA-based vaccines for several kinds of cancer, including non–small cell lung cancer (NSCLC), colorectal cancer, gastroesophageal cancer, urothelial cancer, bladder, head and neck cancer, pancreatic cancer,[118] hepatic cancer, prostate cancer, ovarian, and skin cancer are under evaluation in clinical and preclinical trials.[119] When finding vaccine candidates that can fight *H pylori*, reverse vaccinology is a game-changer. Vaccine development has traditionally relied on growing and then inactivating or weakening a whole pathogen.[120] On the contrary, reverse vaccinology uses bioinformatics and computer study of pathogen genomes to find possible targets for vaccines, which is a different approach.[121] Besides, vaccines developed using this method are exact and safe, and they also have a lower production cost and stronger humoral and cellular immune responses.[122] However, several cancer vaccines have been designed using this reverse vaccinology approach, including breast,[123] ovarian,[124] cervical,[125,126] colorectal,[127] and NSCLC.[128]

Thus, this research focuses on the reverse vaccinology approach for creating an mRNA vaccine to address the pressing general need for a stomach cancer vaccine. On the contrary, a multiepitope vaccine against *H pylori* was designed by Khan et al[129] using reverse vaccinology. This vaccine targeted the CagA, OipA, GroEL, and VacA proteins of the bacterium. Another multiepitope vaccine against *H pylori* was designed by Ghosh et al[108] where they targeted HpaA, FlaA, FlaB, and Omp18 antigenic proteins. Keshri et al[130] developed an in silico–based multiepitope vaccine against *H pylori* where they targeted about 25 proteins of the pathogen and identified B-cell, MHC-II, and IFN-γ-inducing epitopes within these proteins. Currently, no mRNA vaccine candidates are available for stomach cancer. Therefore, our designed vaccines are the first in silico–based mRNA vaccines proposed for stomach cancer treatment.

In the study, dual mRNA vaccines (V1 and V2) were designed from the proteins (CagA, GGT, NapA,

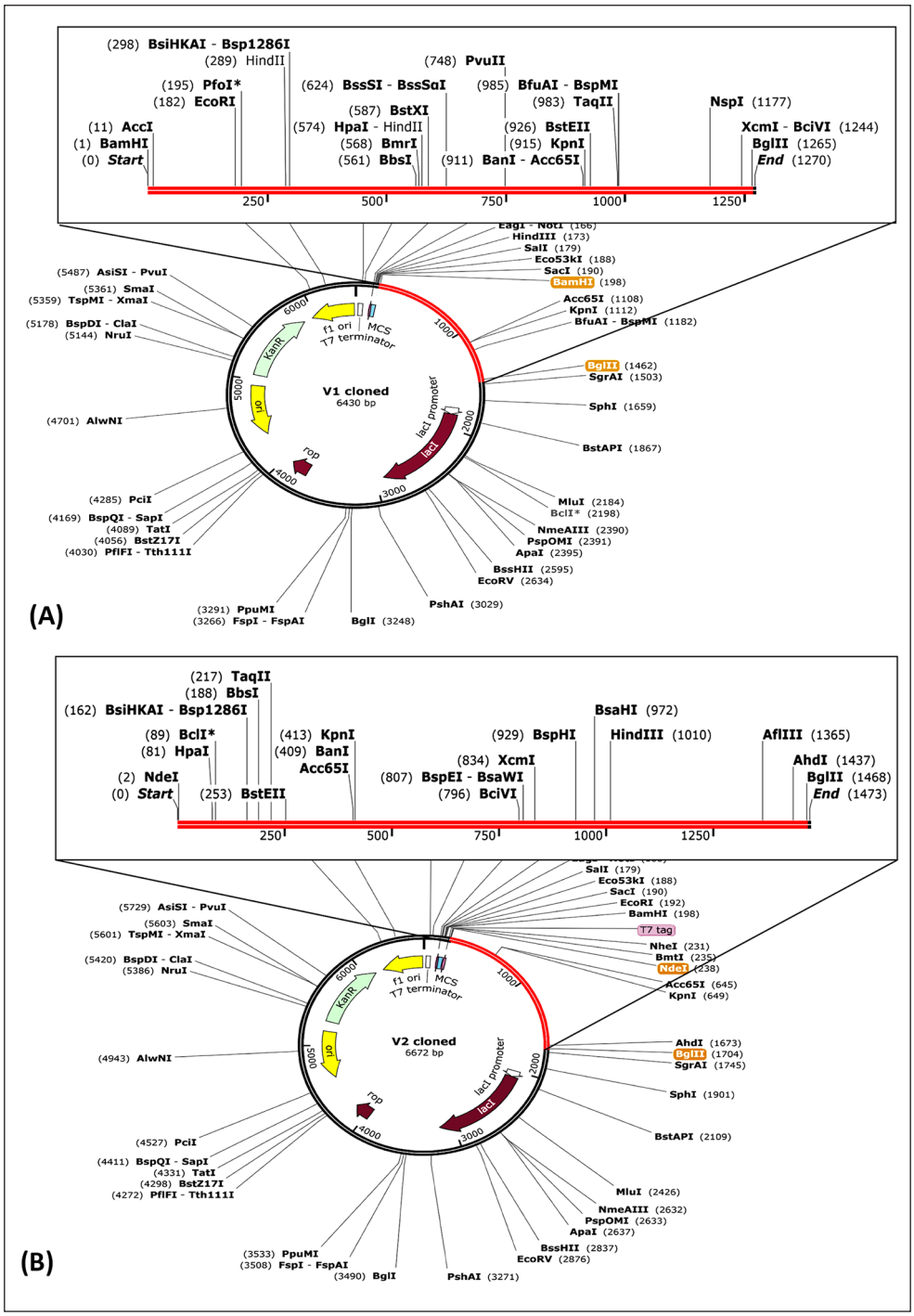

Figure 10. The depiction was about the cloning of (A) V1 and (B) V2 vaccines on suitable vector.

PatA, urease, and VacA) of *H Pylori*. The best epitopes were chosen based on computational methods and used for the construction of vaccines with the incorporation of adjuvants and linkers. Based on biophysical qualities, both vaccines were anticipated to be soluble, potentially exhibiting functional stability under physiological settings.[41] The isoelectric point for V1 was 8.77 and for V2 it was 9.36, indicating that both vaccines were expected to be alkaline. Meanwhile, Sanami et al[125] designed a multiepitope vaccine against human papillomavirus (HPV), where the vaccine was basic in nature with a theoretical pI of 8.33. The vaccines developed by Lu et al[124] had a theoretical pI of 8.64 (breast cancer) and 8.82 (ovarian cancer). Motamedi et al[127] developed the colorectal cancer vaccine with a theoretical pI of 8.13. In our study, the vaccines were predicted to be a stable protein with an instability index of 19.95 for V1 and 36.31 for V2, whereas the HPV, ovarian, and breast vaccines had an instability index of 76.43,[125] 51.52,[124] and 48.43,[124] respectively. Moreover, the aliphatic index of the V1 and V2 were predicted to be 84.33 and 76.23, respectively, indicating the vaccine is a hydrophobic protein containing aliphatic side chains.[41] While the aforementioned HPV, ovarian, breast, and colorectal cancer vaccines had an aliphatic index of 76.43,[125] 76.16,[124] 77.35,[124] and 69.36,[127]

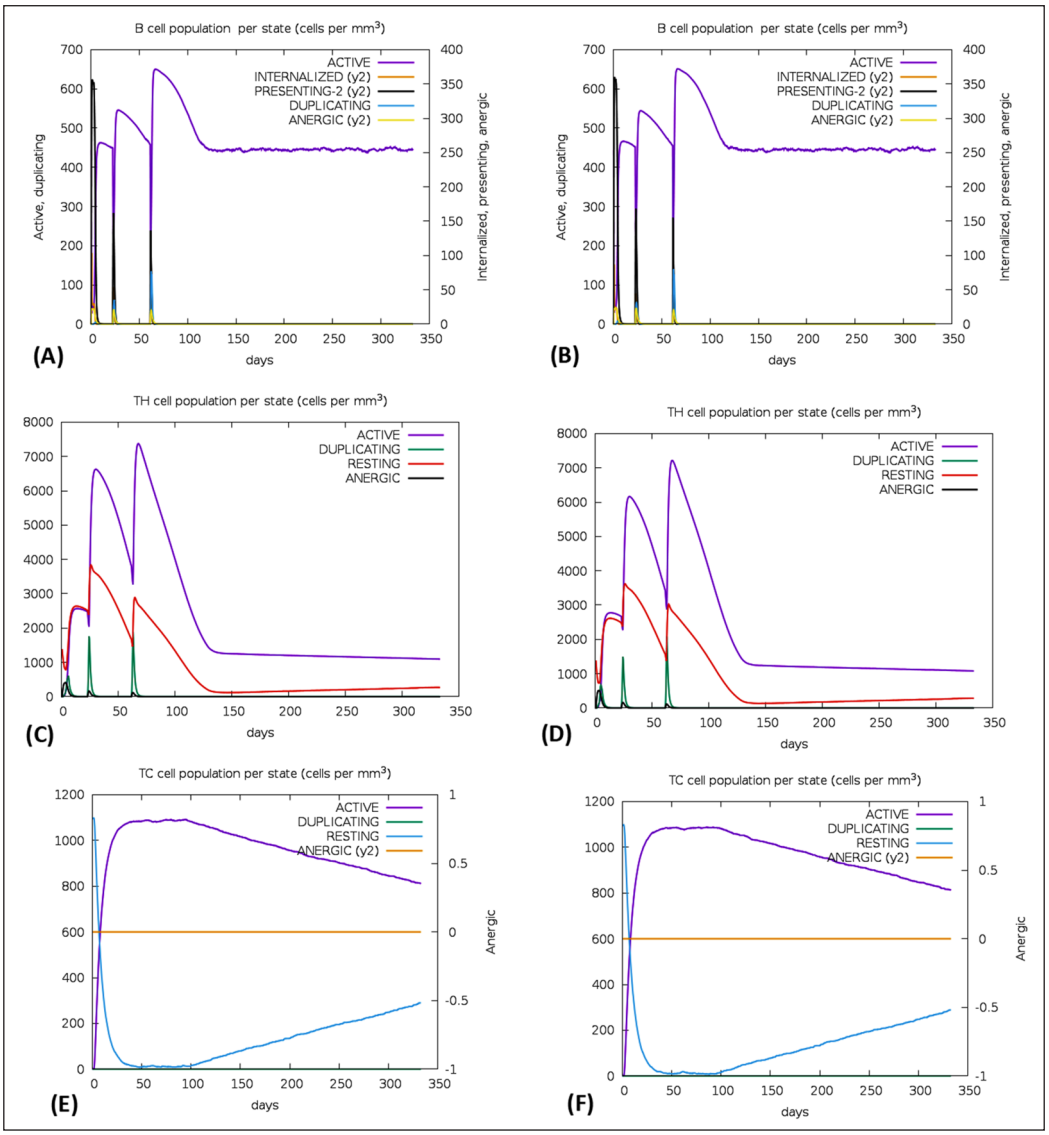

Figure 11. The simulation of the immune system response for V1 and V2. The progression of (A, B) B-cell, (C, D) T_H-cell, (E, F) T_C-cell and cytokine level (G and H) after 3 successive injections of the V1 (A, C, E, and G) and V2 (B, D, F, and H).

respectively. Therefore, the physicochemical properties of our designed mRNA vaccines tend to be similar to the HPV vaccine, which validated the appropriateness of this study.

It is crucial to consider the process of protein folding into its secondary and tertiary structures while developing an effective vaccine.[131] The unfolded and folded proteins' antigens are essential in protein-specific immune responses.[132] Hence, these are the prime targets for antibodies, which in turn mount in response to infections.[133,134] The predicted secondary and tertiary structures of the V1 and V2 were found satisfactory and reliable. The Ramachandran plot analysis also showed that most of the vaccines' residues were within the preferred regions (85.5% for V1% and 88.1% for V2), conferring the structure integrity of the tertiary structures. Contrarily, the HPV and colorectal vaccine had 60.8%[125] and 70.7%[127] amino acid residues in the preferred regions, which indicated that our vaccines exhibited superior 3-dimensional structure compared with theirs.[125] To evaluate the possible association between the vaccines and TLRs on immune cells, a docking analysis was performed using human TLR-2 and TLR-4. According to this analysis, V1 exhibited a substantial affinity toward TLR-2 (lowest energy score of −1132.3 kJ/mol) and TLR-4 (lowest energy score of −1042.7 kJ/mol) receptors, where V2 exhibited a substantial affinity toward TLR-2 (lowest energy score of −1093.6 kJ/ml) and TLR-4 (lowest energy score of −1201.2 kJ/mol) receptors. Meanwhile, the HPV and colorectal vaccines had the lowest energy values of −1103.8 kJ/mol[125] and −1232.7 kJ/mol,[127] respectively. This highlights the accuracy of our prediction strategies and validates the vaccines. The PBDsum indicates that the V1-TLR-2, V2-TLR-4, V2-TLR-2, and V2-TLR-4 complexes contain 7, 22, 10, and 31 hydrogen bonds, respectively.

Subsequently, a simulation of the molecular dynamics was used to verify the structural integrity of the vaccine and its complexes with TLRs. The RMSD of both vaccines and associated TLR complexes indicates dynamic stability during the 50-ns simulation. V1-TLR-4 experiences a consistent increase in RMSD, contrasting V1-TLR-2, which exhibits a gradual

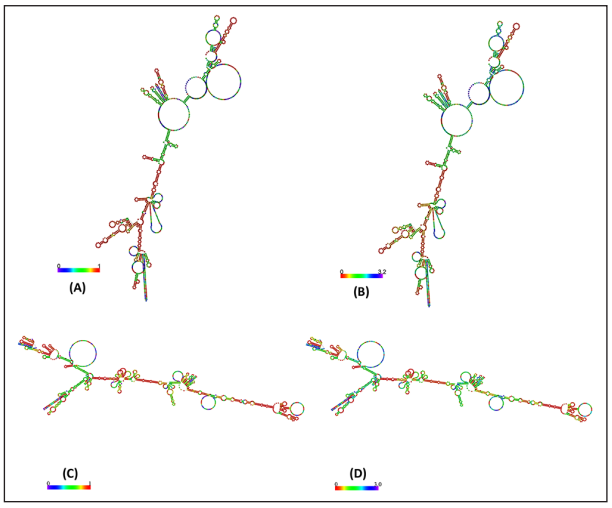

Figure 12. Predicted mRNA structure of the V1 (A and B) and V2 (C and D) by RNAfold web server. The centroid structures of the vaccines with the base pair probabilities (A and C) and the positional entropy (B and D).

decrease in RMSD followed by an initial spike after 10 ns simulation time. V2-TLR-2 and V2-TLR-4 display steady RMSD increments, whereas V1 remains stable. RMSF analysis indicates distinct motility patterns, particularly in C and N terminals. In contrast, Sanami et al[125] achieved only marginal stability in terms of RMSD and RMSF in the HPV vaccine, but only after 30 ns of the operation. Vaccines that we have developed are thus quite effective.

Furthermore, higher Rg values in V1-TLR-4 and V2-TLR-4 suggest increased structural expansion. Notably, SASA values remain insignificantly different throughout the simulations for V1 and V2 complexes, underscoring sustained molecular integrity. This comprehensive evaluation highlights the complex and unique characteristics of both vaccines and docked complexes, offering vital insights into their structural stability, flexibility, compactness, and exposure to solvents throughout the simulation.

The optimization of codon was utilized to evaluate the expression of the vaccines in the *E coli* where the predicted results demonstrated that both vaccines exhibited a significant level of expression in the vector, with the average GC content of the adapted V1 and V2 sequences computed at 51.23% and 51.50%, respectively, while both vaccines attained a CAI value of 1.0 each. Meanwhile, the HPV and colorectal vaccines had an average GC content of 52.04%[125] and 50.180%,[127] while the CAI scores of 0.95[125] and 0.9913,[127] respectively.

We also found a robust and sustained immune response following a 3-dose vaccine regimen for both V1 and V2 vaccines. The increased B-cell populations and prolonged activation of both TH and TC cells indicate the potential for long-lasting immunity, offering enhanced protection against *H pylori*. The V1 mRNA vaccine demonstrates structural stability, as indicated by MFE scores of −487.80 kcal/mol (optimum) and −354.19 kcal/mol (centroid). Similarly, V2 exhibits structural stability with MFE scores of −617.70 kcal/mol (optimum) and −515.48 kcal/mol (centroid). The predicted thermodynamic free energies of −505.96 kcal/mol and −634.92 kcal/mol for the V1 and V2 further support their structural integrity. Remarkably, the ensemble scores of both vaccines predict consistent stability through ingress, transcriptional and expressional activity in the host.

This study highlights the capacity of the dual mRNA vaccines targeting *H pylori* to elicit strong humoral and cellular immune responses, hence addressing stomach cancer. This vaccine will undergo clinical application in laboratories with animals and humans to validate its efficacy. Nevertheless, the present study is computational and hence lacks validation via laboratory studies. Nonetheless, the issue may lie in reconciling computational predictions with experimental findings.

Conclusions

Recognizing the potential of mRNA vaccines, our study focused on designing 2 novel mRNA vaccines, V1 and V2, targeting specific *H pylori* proteins implicated in stomach cancer. We undertook an extensive and meticulous bioinformatics approach to predict epitopes, assess physicochemical properties, and ensure structural stability. The docking analysis indicated substantial affinities between the vaccines and TLRs, while our rigorous molecular dynamics simulations highlighted dynamic stability and structural integrity over a 50-ns timeframe. Codon optimization further confirmed the feasibility of expression in *E coli*, and 3-dose regimens induced robust and sustained immune responses, particularly in the number of B, TH, and TC cells. Structural analyses, including MFE scores and thermodynamic free energies, emphasized the stability of V1 and V2 mRNA structures. Nevertheless, to confirm the safety and effectiveness of vaccines, studies on laboratory, animals, and humans need to be conducted. However, to determine the potentiality of the designed mRNA vaccines, this study establishes a firm groundwork for future research by highlighting the necessity of following experimental validations and clinical investigations.

Acknowledgment

Not applicable

ORCID iDs

Abanti Barua https://orcid.org/0009-0000-2419-7782
Md. Habib Ullah Masum https://orcid.org/0000-0002-0055-1895
Ahmad Abdullah Mahdeen https://orcid.org/0009-0001-6706-8988

Statements and declarations

Ethical considerations

Not applicable

Consent to participate

Not applicable.

Author contributions

Abanti Barua: Conceptualization; Formal analysis; Methodology; Software; Validation; Visualization; Writing—original draft; Writing—review & editing; Supervision.
Md. Habib Ullah Masum: Data curation; Formal analysis; Methodology; Software; Validation; Visualization; Writing—original draft; Writing—review & editing.
Ahmad Abdullah Mahdeen: Data curation; Formal analysis; Methodology; Software; Validation; Visualization; Writing—original draft.

Funding

The author(s) received no financial support for the research, authorship, and/or publication of this article.

Conflicting interests

The author(s) declared no potential conflicts of interest with respect to the research, authorship, and/or publication of this article.

Supplemental material

Supplemental material for this article is available online.

References

1. National Cancer Institute. What is stomach cancer, 2024. Accessed March 21, 2025. https://www.cancer.gov/types/stomach
2. Sung H, Ferlay J, Siegel RL, et al. Global cancer statistics 2020: GLOBOCAN estimates of incidence and mortality worldwide for 36 cancers in 185 countries. *CA Cancer J Clin*. 2021;71:209-249.
3. Cornell WD, Cieplak P, Bayly CI, et al. A second generation force field for the simulation of proteins, nucleic acids, and organic molecules. *J Am Chem Soc*. 1995;117:5179-5197.
4. Floch P, Mégraud F, Lehours P. Helicobacter pylori Strains and Gastric MALT Lymphoma. *Toxins*. 2017;9:132.
5. Khatoon J, Prasad KN, Prakash Rai R, Ghoshal UC, Krishnani N. Association of heterogenicity of Helicobacter pylori cag pathogenicity island with peptic ulcer diseases and gastric cancer. *Br J Biomed Sci*. 2017;74:121-126.
6. Ilic M, Ilic I. Epidemiology of stomach cancer. *World J Gastroenterol*. 2022;28:1187-1203.
7. National Cancer Institute. Cancer stat facts: stomach cancer, 2024. Accessed December 31, 2024. https://seer.cancer.gov/statfacts/html/stomach.html
8. Morgan E, Arnold M, Camargo MC, et al. The current and future incidence and mortality of gastric cancer in 185 countries, 2020-40: a population-based modelling study. *EClinicalMedicine*. 2022;47:101404.
9. Ferlay J, Colombet M, Soerjomataram I, et al. Cancer statistics for the year 2020: An overview. *Int J Cancer*. 2021;149:778–789.
10. Moss SF. The clinical evidence linking Helicobacter pylori to gastric cancer. *Cell Mol Gastroenterol Hepatol*. 2017;3:183-191.
11. Chudasama R, Phung Q, Hsu A, Almhanna K. Vaccines in Gastrointestinal malignancies: from prevention to treatment. *Vaccines*. 2021;9:647.
12. Srivatsan S, Patel JM, Bozeman EN, et al. Allogeneic tumor cell vaccines: the promise and limitations in clinical trials. *Hum Vaccin Immunother*. 2014;10:52-63.
13. Sondak VK, Sabel MS, Mulé JJ. Allogeneic and autologous melanoma vaccines: where have we been and where are we going? *Clin Cancer Res*. 2006;12:2337s-2341s.
14. Gnjatic S, Ritter E, Büchler MW, et al. Seromic profiling of ovarian and pancreatic cancer. *Proc Natl Acad Sci U S A*. 2010;107:5088-5093.
15. Zom GG, Khan S, Filippov DV, Ossendorp F. TLR ligand-peptide conjugate vaccines: toward clinical application. *Adv Immunol*. 2012;114:177-201.
16. Rivoltini L, Castelli C, Carrabba M, et al. Human tumor-derived heat shock protein 96 mediates in vitro activation and in vivo expansion of melanoma- and colon carcinoma-specific T cells. *J Immunol*. 2003;171:3467-3474.
17. Kantoff PW, Schuetz TJ, Blumenstein BA, et al. Overall survival analysis of a phase II randomized controlled trial of a Poxviral-based PSA-targeted immunotherapy in metastatic castration-resistant prostate cancer. *J Clin Oncol*. 2010;28:1099-1105.
18. Travieso T, Li J, Mahesh S, Mello J, Blasi M. The use of viral vectors in vaccine development. *NPJ Vaccines*. 2022;7:75.
19. Hofmann O, Caballero OL, Stevenson BJ, et al. Genome-wide analysis of cancer/testis gene expression. *Proc Natl Acad Sci U S A*. 2008;105:20422-20427.
20. Pan RY, Chung WH, Chu MT, et al. Recent development and clinical application of cancer vaccine: targeting neoantigens. *J Immunol Res*. 2018;2018:4325874.
21. Orlandi F, Guevara-Patiño JA, Merghoub T, Wolchok JD, Houghton AN, Gregor PD. Combination of epitope-optimized DNA vaccination and passive infusion of monoclonal antibody against HER2/neu leads to breast tumor regression in mice. *Vaccine*. 2011;29:3646-3654.
22. Gote V, Bolla PK, Kommineni N, et al. A comprehensive review of mRNA vaccines. *Int J Mol Sci*. 2023;24:2700.
23. Tomb JF, White O, Kerlavage AR, et al. The complete genome sequence of the gastric pathogen Helicobacter pylori. *Nature*. 1997;388:539-547.
24. Winans SC, Burns DL, Christie PJ. Adaptation of a conjugal transfer system for the export of pathogenic macromolecules. *Trends Microbiol*. 1996;4:64-68.
25. Mimuro H, Suzuki T, Tanaka J, Asahi M, Haas R, Sasakawa C. Grb2 is a key mediator of helicobacter pylori CagA protein activities. *Mol Cell*. 2002;10:745-755.
26. Shadifar M, Ataee R, Ataie A, Heydari Gorgi AM, Nasri Nasrabadi N, Nouri S. Genetic and molecular aspects of Helicobacter pylori in gastritis, pre- cancerous conditions and gastric adenocrcinoma. *Gastroenterol Hepatol Bed Bench*. 2015;8:S15-S22.
27. Hatakeyama M. Structure and function of Helicobacter pylori CagA, the first-identified bacterial protein involved in human cancer. *Proc Jpn Acad Ser B Phys Biol Sci*. 2017;93:196-219.
28. Ricci V, Giannouli M, Romano M, Zarrilli R. Helicobacter pylori gamma-glutamyl transpeptidase and its pathogenic role. *World J Gastroenterol*. 2014;20:630-638.
29. Butcher LD, den Hartog G, Ernst PB, Crowe SE. Oxidative stress resulting from Helicobacter pylori infection contributes to gastric carcinogenesis. *Cell Mol Gastroenterol Hepatol*. 2017;3:316-322.
30. Zanotti G, Papinutto E, Dundon W, et al. Structure of the neutrophil-activating protein from Helicobacter pylori. *J Mol Biol*. 2002;323:125-130.
31. Satin B, Del Giudice G, Della Bianca V, et al. The neutrophil-activating protein (HP-NAP) of Helicobacter pylori is a protective antigen and a major virulence factor. *J Exp Med*. 2000;191:1467-1476.

32. Evans DJ Jr, Evans DG, Takemura T, et al. Characterization of a Helicobacter pylori neutrophil-activating protein. *Infect Immun*. 1995;63:2213-2220.
33. Wang G, Maier RJ. An NADPH quinone reductase of Helicobacter pylori plays an important role in oxidative stress resistance and host colonization. *Infect Immun*. 2004;72:1391-1396.
34. Wang G, Lo LF, Forsberg LS, Maier RJ. Helicobacter pylori peptidoglycan modifications confer lysozyme resistance and contribute to survival in the host. *Mbio*. 2012;3:e00409-00412.
35. Mobley HL. The role of Helicobacter pylori urease in the pathogenesis of gastritis and peptic ulceration. *Aliment Pharmacol Ther*. 1996;10:57-64.
36. Valenzuela-Valderrama M, Cerda-Opazo P, Backert S, et al. The Helicobacter pylori urease virulence factor is required for the induction of hypoxia-induced factor-1α in gastric cells. *Cancers*. 2019;11:799.
37. Goda N, Ryan HE, Khadivi B, McNulty W, Rickert RC, Johnson RS. Hypoxia-inducible factor 1alpha is essential for cell cycle arrest during hypoxia. *Mol Cell Biol*. 2003;23:359-369.
38. Comber JD, Philip R. MHC class I antigen presentation and implications for developing a new generation of therapeutic vaccines. *Ther Adv Vaccines*. 2014;2:77-89.
39. Duffy EB, Drake JR, Harton JA. Evolving insights for MHC class II antigen processing and presentation in health and disease. *Curr Pharmacol Rep*. 2017;3:213-220.
40. Unanue ER, Turk V, Neefjes J. Variations in MHC class II antigen processing and presentation in health and disease. *Annu Rev Immunol*. 2016;34:265-297.
41. Bibi S, Ullah I, Zhu B, et al. In silico analysis of epitope-based vaccine candidate against tuberculosis using reverse vaccinology. *Sci Rep*. 2021;11:1249.
42. Patankar YR, Sutiwisesak R, Boyce S, et al. Limited recognition of Mycobacterium tuberculosis-infected macrophages by polyclonal CD4 and CD8 T cells from the lungs of infected mice. *Mucosal Immunol*. 2020;13:140-148.
43. Krocova Z, Plzakova L, Pavkova I, et al. The role of B cells in an early immune response to Mycobacterium bovis. *Microb Pathog*. 2020;140:103937.
44. Rappuoli R, Bottomley MJ, D'Oro U, Finco O, De Gregorio E. Reverse vaccinology 2.0: human immunology instructs vaccine antigen design. *J Exp Med*. 2016;213:469-481.
45. Oli AN, Obialor WO, Ifeanyichukwu MO, et al. Immunoinformatics and vaccine development: an overview. *Immunotargets Ther*. 2020;9:13-30.
46. Nobel Prize. Press release, 2023. Accessed August 14, 2024. https://www.nobelprize.org/prizes/medicine/2023/press-release/
47. National Center for Biotechnology Information. Protein, 2024. Accessed May 20, 2024. https://www.ncbi.nlm.nih.gov/protein/.
48. Reynisson B, Alvarez B, Paul S, Peters B, Nielsen M. NetMHCpan-4.1 and NetMHCIIpan-4.0: improved predictions of MHC antigen presentation by concurrent motif deconvolution and integration of MS MHC eluted ligand data. *Nucleic Acids Res*. 2020;48:W449-w454.
49. MHC-II Binding Predictions, 2024. Accessed March 21, 2025. http://tools.iedb.org/mhcii/
50. Reynisson B, Barra C, Kaabinejadian S, Hildebrand WH, Peters B, Nielsen M. Improved prediction of MHC II antigen presentation through integration and motif deconvolution of mass spectrometry MHC eluted ligand data. *J Proteome Res*. 2020;19:2304-2315.
51. Wang P, Sidney J, Dow C, Mothé B, Sette A, Peters B. A systematic assessment of MHC class II peptide binding predictions and evaluation of a consensus approach. *PLoS Comput Biol*. 2008;4:e1000048.
52. Doytchinova IA, Flower DR. VaxiJen: a server for prediction of protective antigens, tumour antigens and subunit vaccines. *BMC Bioinformatics*. 2007;8:4.
53. Dimitrov I, Bangov I, Flower DR, Doytchinova I., AllerTOP v.2–a server for in silico prediction of allergens. *J Mol Model*. 2014;20:2278.
54. Sharma N, Naorem LD, Jain S, Raghava GPS. ToxinPred2: an improved method for predicting toxicity of proteins. *Brief Bioinform*. 2022;23:bbac174.
55. Designing and prediction of toxic peptides, 2024. Accessed March 21, 2025. http://crdd.osdd.net/raghava/toxinpred/
56. MHC-I binding predictions, 2024. Accessed March 21, 2025. http://tools.immuneepitope.org/mhci/
57. Andreatta M, Nielsen M. Gapped sequence alignment using artificial neural networks: application to the MHC class I system. *Bioinformatics*. 2016;32:511-517.
58. ElliPro: antibody epitope prediction, 2024. Accessed March 21, 2025. http://tools.iedb.org/ellipro/
59. Artificial neural network based B-cell epitope prediction server, 2024. Accessed March 21, 2025. http://crdd.osdd.net/raghava/abcpred/
60. Adhikari UK, Tayebi M, Rahman MM. Immunoinformatics approach for epitope-based peptide vaccine design and active site prediction against polyprotein of emerging oropouche virus. *J Immunol Res*. 2018;2018:6718083.
61. Mahapatra SR, Sahoo S, Dehury B, et al. Designing an efficient multi-epitope vaccine displaying interactions with diverse HLA molecules for an efficient humoral and cellular immune response to prevent COVID-19 infection. *Expert Rev Vaccines*. 2020;19:871-885.
62. Bui HH, Sidney J, Dinh K, Southwood S, Newman MJ, Sette A. Predicting population coverage of T-cell epitope-based diagnostics and vaccines. *BMC Bioinformatics*. 2006;7:153.
63. Masum MHU, Mahdeen AA, Barua L, Parvin R, Heema HP, Ferdous J. Developing a chimeric multiepitope vaccine against Nipah virus (NiV) through immunoinformatics, molecular docking and dynamic simulation approaches. *Microb Pathog*. 2024;197:107098.
64. Mahdeen AA, Hossain I, Masum MHU, Rabbi TMF, Islam S. Designing novel multiepitope mRNA vaccine targeting Hendra virus (HeV): an integrative approach utilizing immunoinformatics, reverse vaccinology, and molecular dynamics simulation. *PLoS ONE*. 2024;19:e0312239.
65. Parvin R, Habib Ullah Masum M, Ferdous J, Mahdeen AA, Shafiqul Islam Khan M. Designing of a chimeric multiepitope vaccine against bancroftian lymphatic filariasis through immunoinformatics approaches. *PLoS ONE*. 2024;19:e0310398.
66. Bioinformatics SSIo. Expasy. ProtParam tool. Accessed May 20, 2024. https://web.expasy.org/protparam/
67. Wilkins MR, Gasteiger E, Bairoch A, et al. Protein identification and analysis tools in the ExPASy server. *Methods Mol Biol*. 1999;112:531-552.
68. Hirokawa T, Boon-Chieng S, Mitaku S. SOSUI: classification and secondary structure prediction system for membrane proteins. *Bioinformatics*. 1998;14:378-379.
69. Magnan CN, Randall A, Baldi P. SOLpro: accurate sequence-based prediction of protein solubility. *Bioinformatics*. 2009;25:2200-2207.
70. Mitaku S, Hirokawa T. Physicochemical factors for discriminating between soluble and membrane proteins: hydrophobicity of

helical segments and protein length. *Protein Eng*. 1999;12:953-957.
71. Mitaku S, Hirokawa T, Tsuji T. Amphiphilicity index of polar amino acids as an aid in the characterization of amino acid preference at membrane-water interfaces. *Bioinformatics*. 2002;18:608-616.
72. Sopma Secondary Structure Prediction Method, 2024. Accessed March 21, 2025. https://npsa-prabi.ibcp.fr/cgi-bin/npsa_automat.pl?page=/NPSA/npsa_sopma.html
73. Dimitrov I, Naneva L, Doytchinova I, Bangov I. AllergenFP: allergenicity prediction by descriptor fingerprints. *Bioinformatics*. 2013;30:846-851.
74. Maurer-Stroh S, Krutz NL, Kern PS, et al. AllerCatPro-prediction of protein allergenicity potential from the protein sequence. *Bioinformatics*. 2019;35:3020-3027.
75. Saha S, Raghava GP. AlgPred: prediction of allergenic proteins and mapping of IgE epitopes. *Nucleic Acids Res*. 2006;34:W202-W209.
76. VaxiJen: a server for prediction of protective antigens, tumour antigens and subunit vaccines, 2007.
77. GOR IV secondary structure prediction method, 2024. Accessed March 21, 2025. https://npsa-prabi.ibcp.fr/cgi-bin/npsa_automat.pl?page=/NPSA/npsa_gor4.html
78. Buchan DWA, Jones DT. The PSIPRED protein analysis workbench: 20 years on. *Nucleic Acids Res*. 2019;47:W402-W407.
79. Combet C, Blanchet C, Geourjon C, Deléage G. NPS@: network protein sequence analysis. *Trends Biochem Sci*. 2000;25:147-150.
80. Jones DT. Protein secondary structure prediction based on position-specific scoring matrices. *J Mol Biol*. 1999;292:195-202.
81. I-TASSER, 2024. Accessed March 21, 2025. https://zhanggroup.org/I-TASSER/
82. Ko J, Park H, Heo L, Seok C. GalaxyWEB server for protein structure prediction and refinement. *Nucleic Acids Res*. 2012;40:W294-297.
83. Laskowski R, Macarthur MW, Moss DS, Thornton J. PROCHECK: a program to check the stereochemical quality of protein structures. *J Appl Crystallogr*. 1993;26:283-291.
84. Laskowski RA, MacArthur MW, Thornton JM. PROCHECK: validation of protein-structure coordinates. *Int Table Crystallogr*. 2012;F:684-687.
85. Laskowski RA, Rullmannn JA, MacArthur MW, Kaptein R, Thornton JM. AQUA and PROCHECK-NMR: programs for checking the quality of protein structures solved by NMR. *J Biomol NMR*. 1996;8:477-486.
86. Morris AL, MacArthur MW, Hutchinson EG, Thornton JM. Stereochemical quality of protein structure coordinates. *Proteins*. 1992;12:345-364.
87. Kringelum JV, Lundegaard C, Lund O, Nielsen M. Reliable B cell epitope predictions: impacts of method development and improved benchmarking. *PLoS Comput Biol*. 2012;8:e1002829.
88. Ponomarenko J, Bui HH, Li W, et al. ElliPro: a new structure-based tool for the prediction of antibody epitopes. *BMC Bioinformatics*. 2008;9:514.
89. Zhu F, Tan C, Li C, et al. Design of a multi-epitope vaccine against six Nocardia species based on reverse vaccinology combined with immunoinformatics. *Front Immunol*. 2023;14:1100188.
90. Gong Z, Zhang J, Zhang S, et al. TLR2, TLR4, and NLRP3 mediated the balance between host immune-driven resistance and tolerance in Staphylococcus aureus-infected mice. *Microb Pathog*. 2022;169:105671.
91. Kozakov D, Beglov D, Bohnuud T, et al. How good is automated protein docking. *Proteins*. 2013;81:2159-2166.
92. Kozakov D, Hall DR, Xia B, et al. The ClusPro web server for protein-protein docking. *Nat Protoc*. 2017;12:255-278.
93. Pictorial database of 3D structures in the Protein Data Bank, 2024. Accessed March 21, 2025. https://www.ebi.ac.uk/thornton-srv/databases/pdbsum/
94. Abraham MJ, Murtola T, Schulz R, et al. GROMACS: high performance molecular simulations through multi-level parallelism from laptops to supercomputers. *SoftwareX*. 2015;1-2:19-25.
95. Java Codon Adaptation tool, 2024. Accessed March 21, 2025. https://www.jcat.de/
96. Vinogradov AE. Dualism of gene GC content and CpG pattern in regard to expression in the human genome: magnitude versus breadth. *Trends Genet*. 2005;21:639-643.
97. Chan CY, Carmack CS, Long DD, et al. A structural interpretation of the effect of GC-content on efficiency of RNA interference. *BMC Bioinformatics*. 2009;10:S33.
98. Rapin N, Lund O, Bernaschi M, Castiglione F. Computational immunology meets bioinformatics: the use of prediction tools for molecular binding in the simulation of the immune system. *PLoS ONE*. 2010;5:e9862.
99. Leong DP, Zhang A, Breznik JA, et al. Comparison of three dosing intervals for the primary vaccination of the SARS-CoV-2 mRNA Vaccine (BNT162b2) on magnitude, neutralization capacity and durability of the humoral immune response in health care workers: a prospective cohort study. *PLoS ONE*. 2023;18:e0281673.
100. Liu J, Huang B, Li G, et al. Immunogenicity and Safety of a 3-dose regimen of a SARS-CoV-2 inactivated vaccine in adults: a randomized, double-blind, placebo-controlled Phase 2 trial. *J Infect Dis*. 2021;225:1701-1709.
101. Gruber AR, Lorenz R, Bernhart SH, Neuböck R, Hofacker IL. The Vienna RNA websuite. *Nucleic Acids Res*. 2008;36:W70-W74.
102. Lorenz R, Bernhart SH, Höner zu, Siederdissen C, et al. ViennaRNA package 2.0. *Algorithm Mol Bio*. 2011;6:26.
103. Motamedi H, Alvandi A, Fathollahi M, et al. In silico designing and immunoinformatics analysis of a novel peptide vaccine against metallo-beta-lactamase (VIM and IMP) variants. *PLoS ONE*. 2023;18:e0275237.
104. Transcription and translation tool, 2025. Accessed February 11, 2025. https://biomodel.uah.es/en/lab/cybertory/analysis/trans.htm
105. Sutton P, Boag JM. Status of vaccine research and development for Helicobacter pylori. *Vaccine*. 2019;37:7295-7299.
106. Friedrich V, Gerhard M. Vaccination against Helicobacter pylori: an approach for cancer prevention. *Mol Aspects Med*. 2023;92:101183.
107. Paranthaman P, Veerappapillai S. Design of a potential Sema4A-based multi-epitope vaccine to combat triple-negative breast cancer: an immunoinformatic approach. *Med Oncol*. 2023;40:105.
108. Ghosh P, Bhakta S, Bhattacharya M, et al. A novel multi-epitopic peptide vaccine candidate against Helicobacter pylori: in-silico identification, design, cloning and validation through molecular dynamics. *Int J Pept Res Ther*. 2021;27:1149-1166.
109. Parvizpour S, Pourseif MM, Razmara J, Rafi MA, Omidi Y. Epitope-based vaccine design: a comprehensive overview of bioinformatics approaches. *Drug Discov Today*. 2020;25:1034-1042.
110. Chen HZ, Tang LL, Yu XL, Zhou J, Chang YF, Wu X. Bioinformatics analysis of epitope-based vaccine design

against the novel SARS-CoV-2. *Infect Dis Poverty*. 2020;9:88.
111. Higashihara Y, Kato J, Nagahara A, et al. Phase I clinical trial of peptide vaccination with URLC10 and VEGFR1 epitope peptides in patients with advanced gastric cancer. *Int J Oncol*. 2014;44:662-668.
112. Ishikawa H, Imano M, Shiraishi O, et al. Phase I clinical trial of vaccination with LY6K-derived peptide in patients with advanced gastric cancer. *Gastric Cancer*. 2014;17:173-180.
113. Moss SF, Moise L, Lee DS, et al. HelicoVax: epitope-based therapeutic Helicobacter pylori vaccination in a mouse model. *Vaccine*. 2011;29:2085-2091.
114. Li Y, Chen Z, Ye J, et al. Antibody production and Th1-biased response induced by an epitope vaccine composed of cholera toxin B unit and Helicobacter pylori Lpp20 epitopes. *Helicobacter*. 2016;21:234-248.
115. Sutton P. At last, vaccine-induced protection against Helicobacter pylori. *Lancet*. 2015;386:1424-1425.
116. Zeng M, Mao X-H, Li J-X, et al. Efficacy, safety, and immunogenicity of an oral recombinant Helicobacter pylori vaccine in children in China: a randomised, double-blind, placebo-controlled, phase 3 trial. *The Lancet*. 2015;386:1457-1464.
117. Mohammadi Y, Nezafat N, Negahdaripour M, Eskandari S, Zamani M. In silico design and evaluation of a novel mRNA vaccine against BK virus: a reverse vaccinology approach. *Immunol Res*. 2023;71:422-441.
118. Balachandran VP, Rojas LA, Sethna Z, et al. Phase I trial of adjuvant autogene cevumeran, an individualized mRNA neoantigen vaccine, for pancreatic ductal adenocarcinoma. 2022;40:2516-2516.
119. Wang B, Pei J, Xu S, Liu J, Yu J. Recent advances in mRNA cancer vaccines: meeting challenges and embracing opportunities. *Front Immunol*. 2023;14:1246682.
120. Moxon R, Reche PA, Rappuoli R. Editorial: reverse vaccinology. *Front Immunol*. 2019;10:2776.
121. Kanampalliwar AM. Reverse vaccinology and its applications. *Methods Mol Biol*. 2020;2131:1-16.
122. Zhang L. Multi-epitope vaccines: a promising strategy against tumors and viral infections. *Cell Mol Immunol*. 2018;15:182-184.
123. Parvizpour S, Razmara J, Pourseif MM, Omidi Y. In silico design of a triple-negative breast cancer vaccine by targeting cancer testis antigens. *BioImpacts*. 2019;9:45-56.
124. Lu L, Ma W, Johnson CH, Khan SA, Irwin ML, Pusztai L. In silico designed mRNA vaccines targeting CA-125 neoantigen in breast and ovarian cancer. *Vaccine*. 2023;41:2073-2083.
125. Sanami S, Azadegan-Dehkordi F, Rafieian-Kopaei M, et al. Design of a multi-epitope vaccine against cervical cancer using immunoinformatics approaches. *Sci Rep*. 2021;11:12397.
126. Sanami S, Rafieian-Kopaei M, Dehkordi KA, et al. In silico design of a multi-epitope vaccine against HPV16/18. *BMC Bioinformatics*. 2022;23:311.
127. Motamedi H, Ari MM, Shahlaei M, et al. Designing multi-epitope vaccine against important colorectal cancer (CRC) associated pathogens based on immunoinformatics approach. *BMC Bioinformatics*. 2023;24:65.
128. Rahman MM, Masum MHU, Talukder A, Akter R. An in silico reverse vaccinology approach to design a novel multiepitope peptide vaccine for non-small cell lung cancers. *Inform Med Unlocked*. 2023;37:101169.
129. Khan M, Khan S, Ali A, et al. Immunoinformatics approaches to explore Helicobacter Pylori proteome (Virulence Factors) to design B and T cell multi-epitope subunit vaccine. *Sci Rep*. 2019;9:13321.
130. Keshri AK, Kaur R, Rawat SS, et al. Designing and development of multi-epitope chimeric vaccine against Helicobacter pylori by exploring its entire immunogenic epitopes: an immunoinformatic approach. *BMC Bioinformatics*. 2023;24:358.
131. Rajendran Krishnamoorthy H, Karuppasamy R. Designing a novel SOX9 based multi-epitope vaccine to combat metastatic triple-negative breast cancer using immunoinformatics approach. *Mol Divers*. 2023;27:1829-1842.
132. Paranthaman P, Veerappapillai S. Tackling suppressive cancer microenvironment by NARF-derived immune modulatory vaccine and its validation using simulation strategies. *Front Phys*. 2024;12:1342115.
133. Scheiblhofer S, Laimer J, Machado Y, Weiss R, Thalhamer J. Influence of protein fold stability on immunogenicity and its implications for vaccine design. *Expert Rev Vaccines*. 2017;16:479-489.
134. Krishnamoorthy HR, Karuppasamy R. Design and in silico validation of a novel MZF-1-based multi-epitope vaccine to combat metastatic triple negative breast cancer. *Vaccines*. 2023;11:577.